Charles University

Faculty of Science

Study programme: Biology

Branch of study: Cell and Developmental Biology

Bc. Jakub Onhajzer

Regenerative potential of Sertoli cell progenitors regarding heart injury in *Xenopus tropicalis*

Regenerační potenciál progenitorů Sertoliho buněk v rámci poškození srdce u *Xenopus tropicalis*

Diploma thesis

Supervisor: doc. RNDr. Ing. Vladimír Krylov, Ph.D.

Prague, 2020

Prohlášení

Prohlašuji, že jsem závěrečnou práci zpracoval samostatně a že jsem uvedl všechny použité informační zdroje a literaturu. Tato práce ani její podstatná část nebyla předložena k získání jiného nebo stejného akademického titulu.

V Praze, 31.5.2020

Jakub Onhajzer

.....

Poděkování

Přednostně bych chtěl poděkovat svému školiteli doc. RNDr. Ing. Vladimíru Krylovovi, Ph.D., za jeho trpělivost, spolupráci, ochotu a odborné rady při zpracování této práce. Poděkovaní patří i M.Sc. Thi Minh Xuan Nguyen, Ph.D., a RNDr. Tereze Tlapákové, Ph.D., za jejich odbornou pomoc, velkou dávku motivace a pomoc při práci. Dále bych rád poděkoval Bc. Anetě Wróblové, Bc. Lucii Slovákové, Ing. Mgr. Jiřímu Vávrovi, Mgr. Andree Mančíkové, Mgr. Markétě Vegrichtové, Ing. Martinu Knytlovi, Ph.D., Mgr. Aleši Petelákovi, Ph.D., Bc. Michaele Červenkové a Janě Dvořákové za jejich pomoc a velké množství zážitků. Nakonec děkuji svojí rodině, přítelkyni a kamarádům za veškerou podporu.

Abstrakt

Celosvětově je srdeční selhání jednou z hlavních příčin úmrtí. Léčebný přístup, který by nahradil současný invazivní postup (transplantace s následnou imunosupresivní terapií), v současnosti není k dispozici. Výsledky výzkumu terapie mezenchymálními kmenovými buňkami (MSCs), jasně demonstrují jejich imunomodulační potenciál, který podporuje regeneraci různých orgánů bez nutnosti další podpůrné léčby.

V naší laboratoři byla založena buněčná kultura z varlat juvenilního samce *Xenopus tropicalis* s názvem *Xenopus tropicalis* immature Sertoli cells (XtiSCs). Tyto buňky mají schopnost modulovat imunitní systém, a po ošetření inhibitorem glykogen syntázy kinázy-3 (GSK-3) CHIR99021 diferencují do kardiomyocytů. Mikroinjekcí takto ošetřených buněk do srdce pulce jsme potvrdili jejich přežití a proliferaci po celou dobu pozorování (30 dní). Na druhou stranu, po přímé injekci buněk do srdce dospělé žáby s následovným poškozením myokardu nebyly v oblasti rány lokalizovány žádné buňky. Z tohoto důvodu jsme změnili experimentální přístup a zaměřili se na nepřímý vliv XtiSC (remote control) na regeneraci srdce pomocí produkovaných růstových faktorů. V této souvislosti jsme upustili od ošetření buněk CHIR99021. XtiSCs byly injikovány do kosterního svalu zadní končetiny, kde bez problémů přežívaly a proliferovaly. Svalová injekce buněk 3 dny před poškozením srdce, měla za následek významné snížení hladin fibronektinu a zvýšení množství srdeční svaloviny (kardiomyocytů) 7 dní po poškození. Dále jsme optimalizovali přípravu histologických řezů srdce třemi různými technikami: vibratom, mikrotom a kryotom. Kryotom vykázal nejlepší výsledky z pohledu zachování struktury tkáně a antigenicity.

Stejně jako MSCs, vykazují i Sertoliho buňky slibný způsob modulace imunitní odpovědi po srdečním poškození směrem od zánětu k regeneraci. Navíc terapie pomocí XtiSCs významně redukovala úroveň fibrózy po poranění srdce dospělých jedinců *X. tropicalis*. Sertoliho buňky tak představují slibný zdroj buněk pro účely regenerativní medicíny.

Klíčová slova: srdce, regenerace, Sertoliho buňky, *Xenopus tropicalis*

Abstract

Cardiac failure is one of the leading cause of deaths worldwide. Potential therapeutic approach, which overcome invasive organ transplantation and delivery of immunosuppressive drugs, is lacking nowadays. However, research of mesenchymal stem cells (MSCs) therapy displays immunomodulation potential, which can further promote variety of organ regeneration without need of drug treatment.

Xenopus tropicalis immature Sertoli cells (XtiSCs) culture was established in our laboratory from juvenile *Xenopus tropicalis* male. XtiSCs possess immunomodulatory capacity and differentiation to cardiomyocytes after the treatment with the inhibitor of glycogen synthase kinase-3 (GSK-3) CHIR99021. To test the survival rate of transplanted XtiSCs we firstly microinjected treated cells directly inside tadpole´s heart. XtiSCs proliferated there for the whole tested time period (30 days). However, after direct heart XtiSCs injection and subsequent cardiac injury in adult frog, no cells were localized in wound area. Thus, we focused on remote control of cardiac regeneration using XtiSCs without CHIR99021 treatment. We injected cells inside skeletal muscle bed and confirmed their survival and proliferation. Moreover, if cells were transplanted 3 days before heart injury, it resulted in significant reduction of fibronectin deposition levels and increase in cardiac muscle levels within 7 days after heart injury. We further optimized preparation of heart sections by three different techniques: vibratome, microtome, and cryotome. Cryotome displayed the best results in structure and antigenicity preservation.

Just like MSCs, Sertoli cells display promising way to modulate immune response after cardiac injury by secretion of paracrine and growth factor. Moreover, by significant reduction of fibrosis, XtiSCs treatment may promote cardiac regeneration in adult *X. tropicalis* and Sertoli cells may be new promising source of cells for regenerative medicine.

Key words: heart, regeneration, Sertoli cells, *Xenopus tropicalis*

Content

1 ABBREVIATIONS

AEC	Apical epithelial cap
AER	Apical ectodermal ridge
Akt	protein kinase B
AMH	anti-Müllerian hormone
BSA	Bovine serum albumin
BTB	Blood-testis barrier
C5a	Complement component 5a
Ccnd2	Cyclin D2
Cdk4	Cyclin-dependent kinase 4
Cmlc2	Cardiomyocyte-specific myosin light chain 2
CPCs	Cardiac progenitor cells
CSCs	Cardiac stem cells
DAMPs	Danger-associated molecular patterns
DPA	Days post amputation
DPI	Days post injury
DTA	Diphtheria toxin A
DTR	Diphtheria toxin receptor
ECM	Extracellular matrix
EMT	Epithelial-mesenchymal transition
ET-1	Endothelin-1
FACS	Fluorescence-activated cell sorter
FBS	Foetal bovine serum
FGF 1	Fibroblast growth factor 1
FGF 2	Fibroblast growth factor 2
GSK-3	Glycogen synthase kinase 3
hCG	Human chorionic gonadotropin
HGF	Hepatocyte growth factor
HLA-DR	Human leukocyte antigen-DR

HMGB1	High-mobility group box 1
ICAM-1	Intercellular adhesion molecule 1
IDO	Indoleamine 2,3-dioxygenase
IFNγ	Interferon gamma
IGF-II	Insulin-like growth factor II
IL-10	Interleukin 10
IL-12	Interleukin 12
IL-1α	Interleukin 1 alpha
IL-1β	Interleukin 1 beta
IL-6	Interleukin 6
IL-8	Interleukin 8
iNOS	inducible Nitric oxide synthase
IVF	In vitro fertilization
Klf4	Kruppel-like factor 4
LC-MS	Liquid chromatography–mass spectrometry
LIF	Leukemia inhibitory factor
M-CSF	Macrophage colony-stimulating factor
MEMFA	MOPS + EGTA + Magnesium sulphate + Formaldehyde buffer
MI	Myocardial infarction
MMPs	Matrix metalloproteinases
MMR	Marc's Modified Ringer's solution
mRNA	Messenger ribonucleic acid
MSCs	Mesenchymal stem cells
MyD-88	Myeloid-differentiation primary response protein 88
Mylk3	Myosin light chain kinase 3
Mypn	Myopalladin
NGAL	Neutrophil gelatinase-associated lipocalin
NTR	Nitroreductase
OCT4	Octamer-binding transcription factor 4
PBS	Phosphate-buffered saline

PGE2	Prostaglandin E2
PH3	Phospho-histone H3
RAGE	Receptor for advanced glycation end products
RFP	Red fluorescent protein
ROS	Reactive oxygen species
RPM	Revolutions per minute
RT-PCR	Reverse transcription polymerase chain reaction
SDF-1	Stromal cell derived factor-1
Sox2	Sex determining region Y box 2
TACAS	Thinlayer Advanced Cytology Assay System
Tert	Telomerase reverse transcriptase
TLAQ	TrueBlack lipofuscin autofluorescence quencher
TLRs	Toll-like receptors
TNB	Tris-NaCl-Blocking buffer
TNF-α	Tumor necrosis factor alpha
TnnT	Cardiac troponin T
Ttn	Titin
VEGF	Vascular endothelial growth factor
XtiSCs	*Xenopus tropicalis* immature Sertoli cells
Yap	Yes-associated protein
α-SA	Alpha skeletal muscle actin

2 INTRODUCTION

People are fascinated by complete tissue and organ regeneration from early observations of Prometheus, Spallanzani, and Trembley. However, modern approach in regenerative medicine and tissue engineering began only 30 years ago.

Regenerative medicine may be defined as the potential process of healing or replacing cells, tissues and organs damaged by age, disease, or injury, along with congenital malformations. Nowadays, data displays wide range of available treatment for both, chronic diseases or acute lesions, such as muscular disorders, epithelial or dermal wounds and cardiovascular traumas (Jaklenec *et al.*, 2012). The current approach in therapy of tissue and organ failure is based on allogenic tissue or organ transplantation. However, such transplantations are accompanied with severe immune response and rejection of a transplant, if immunosuppressive drugs are not delivered. On the other hand, these obstacles could be eliminated with a therapeutic approach of MSCs delivery and its immunomodulatory capacity (reviewed in Gallina *et al.*, 2015).

The initial focus of regenerative medicine uses approach of created *de novo* organ transplantation for damaged tissue in the body. Other strategies include the use of nanomaterials and stem cells, which effectively substitute, structure and function of a lost tissue (reviewed in Bajaj *et al.*, 2014). The body´s immune system plays a key role in tissue regeneration after damage. Immune cell recruitment and inflammation are first signs of injury. These pathways help to promote debris and extracellular matrix (ECM) clearance from wound area and further activate signalling molecules that induce dedifferentiation, cell proliferation, and differentiation programs required for successful regeneration. However, increased immune reaction can downregulate or totally inhibit regeneration process, since balanced immune response with a recruitment of an appropriate quantity of immune cells is needed. Furthermore, stem cells used in regenerative medicine, can modulate immune system and improve tissue remodelling.

3 LITERARY OVERVIEW

3.1 Types of regeneration

3.1.1 Epimorphosis

Regenerative capacity of amphibian embryos reaches almost perfect compensation for a lost tissue structure and function. Nevertheless, during metamorphosis and adulthood, such a capacity is lost. Thus, amphibians are great model organisms for a study of regeneration process. They possess remarkable regenerative capacity during early hind limb development. Limb regeneration displays wide range of molecular and cellular pathways, characteristic features for the epimorphosis (Satoh *et al.*, 2005).

Epimorphic regeneration is not only property of amphibian (Zhang *et al.*, 2018), but has been also extensively studied in reptiles (Lozito & Tuan, 2016), salamanders (Kragl *et al.*, 2009), newts (Sandoval-Guzmán *et al.*, 2014) and zebrafish (Jopling *et al.*, 2010). During this process, immediately after injury, wound closure is visible by rapid reepithelization with migratory epidermal cells from wound periphery. Four days post injury (dpi) wound epithelium is created and underneath degradation of debris and ECM starts (Hay and Fischman, 1961). Further, matrix metalloproteinases are secreted and wound epithelium thickens and apical epithelial cap (AEC) is formed from this epithelium (Yang *et al.*, 1999). AEC shares many features with apical ectodermal ridge (AER) in embryonal limb development. So limb regeneration can be divided in two phases, in which the first, early phase is characteristic only for a limb regeneration with the specialized signalling pathways after injury and the second, later stage where similarities could be find with early limb development (reviewed in Bryant *et al*., 2002). The undamaged cells underneath the AEC, such as fibroblast, cartilage, bone, muscle satellite cells, etc. undergo dedifferentiation process and lose intercellular junctions and become separated mesenchymal cells. These cells together with the newly migrated progenitor cells form a mass of undifferentiated cells called a blastema (Sousa *et al.*, 2011). AEC signalling regulates formation and proliferation of a blastema (Thornton, 1960). The blastema cells proliferate, and injured limb is growing distally from a body.

During epimorphosis, a scar-free regeneration occurs and the blastema cells differentiate into all cell types found in a fully functional limb (Delorme *et al.*, 2012).

3.1.2 Compensatory regeneration (hyperplasia)

Characteristic features of compensatory regeneration are hypertrophy (expansion in cell size) and hyperplasia (increase of cell quantity) of remaining cells after organ injury. We could observe this ability within liver regeneration, after chemical injury or partial resection. After injury, a metabolic capacity of liver is limited, and remaining hepatocytes compensate it with restoration of a full liver size. Regenerated liver loses its characteristic anatomical shape, but metabolic activity is well-preserved (reviewed in Mao *et al.*, 2015).

In contrast with, epimorphosis, liver regeneration does not involve typical regeneration stages, such as dedifferentiation, blastema formation, and differentiation. On the other hand, undamaged hepatocytes undergo cell cycle entry, cell proliferation, and termination. Where termination serves as a key step for carcinogenesis prevention. Together, carefully balanced levels of mitogenic and proliferation-inhibiting factors are needed for successful liver regeneration (reviewed in Mao *et al.*, 2015).

3.1.3 Morphallaxis

A typical representative for this kind of regeneration is Hydra. Hydra´s body structure is rather simple with only one axis with radial symmetry, which consists of head, body column, and foot.

Morphallaxis is a type of a regenerative process where a blastema is not formed and yet, when Hydra is cut in two, it forms two independent organisms. In this process tissue remodelling occurs without cell dedifferentiation. On the other hand, Hydra´s body contains activation and inhibition gradients of morphogens. Morphogen gradients play a crucial role in early embryogenesis in a huge number of metazoans, where they launch and establish axial pattering. However, in Hydra, these gradients are also continuously active in adult and they provide positional information for cells in a body. Main sources of morphogens gradients are head (hypostome) and foot (basal disc) (Cohen & MacWilliams, 1975). Head activation gradient together with basal disc activation gradient control the length of the body axis of a Hydra. Moreover, these regions also produce inhibition gradients

which provide just a one head and a one foot formation in a body axis. Altogether, gradients in the middle of an axis has balanced levels and body column is created. Thus, when Hydra is cut or injured, cells have a positional information and with a process of tissue remodelling, they can regenerate and create two independent organisms (reviewed in Agata *et al.*, 2007).

3.2 Heart regeneration in model organisms

Since, myocardial infarction (MI) flowed by cardiac failure, is a major cause of morbidity and mortality (World Health Organisation, 2018), regeneration research in a vital organ like the heart, is highly clinically relevant. Lower vertebrates such as zebrafish and axolotl exhibit extraordinary regenerative capacity of lost cardiac tissue (Cano-Martínez *et al.*, 2010; Jopling *et al.*, 2010). In contrast, adult *Xenopus laevis* loses its regenerative capacity after metamorphosis (Marshall *et al.*, 2017, 2019). Moreover, adult mammals are not capable to fully restore structure and function of damaged heart, because adult mammalian cardiac cells are incapable of cell cycle entry and division. As an alternative, lost cardiac tissue is compensated with scar tissue. Further, contractility and heart function are weakened and it can leads to cardiac failure and death (reviewed in Porrello & Olson, 2014). However, latest research by Porrello *et al.* (2011, 2013) showed, that neonatal mouse is capable to regenerate damaged heart after partial surgical resection until 7 days after birth. This regeneration exhibit cardiomyocyte proliferation with low fibronectin and scar deposition. Next, Bergmann *et al.* (2009, 2015) observed human cardiomyocyte turnover, with ^{14}C integrated into DNA, during the Cold War nuclear bomb testing. They used this advantage, to characterize cardiomyocytes age, and claimed, that around 50 % of all human cardiomyocytes are changed during lifetime. Thus, observing molecular and cellular pathways of cardiac regeneration, and application of possible treatments are going to be one of the main scientific and clinical goals in future. First of all, new and possible treatments need to be characterized and tested on model organisms with wide range of regenerative capacities.

3.2.1 Techniques for studying heart regeneration and repair

In the scientific field of heart regeneration, four main injury models were established. Cardiac damage can be achieved by resection (Poss *et al.*, 2002) , cryoinjury (Yu *et al*., 2018), genetic ablation (Wang *et al.*, 2011) and ligation of coronary artery (Haubner *et al.*, 2012) (Fig. 1). Resection together with cryoinjury and genetic ablation are useful methods for smaller animals. On the other hand, coronary ligation is useful approach in rodents and larger animals, because of better accessibility of arteries. This technique best mimics MI in human (Haubner *et al.*, 2012). However, heart injury technique is not specific for a type of model organism, but rather based on equipment availability in laboratory.

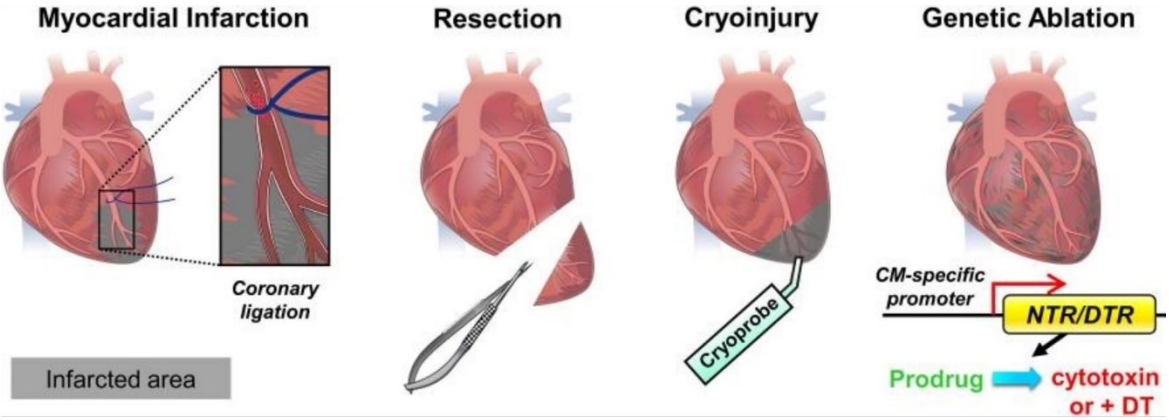

Figure 1. Illustration of the heart injury models:
Coronary ligation of the left anterior descending coronary artery generates localized ischemic area of cell death, followed by MI. For removing the part of cardiac muscle without a vast area of necrotic tissue, resection is used. Cryoinjury is performed via cryoprobe tempered in liquid nitrogen, which is applied to ventricle. Method of genetic ablation modifies DNA transcription in cardiomyocyte-specific manner. Where cardiomyocyte-specific nitroreductase (NTR) or Diphtheria toxin receptor (DTR) converts a non-toxic prodrug into cytotoxic product, which induces cell death (adopted from Lai *et al.*, 2019).

Resection as a heart injury model is simple to manage with good reproducibility of damaged area. On the other hand, interpretation to human MI is complicated due to removal of cardiac tissue with resection. Resection does not involve any ischemia-specific area with local cell death, what is common result of MI in mammals. Resection in zebrafish rather involves blood clot formation, fibronectin and collagen deposition with less necrosis (Poss *et al.*, 2002).

Relatively similar mechanisms to MI could be triggered by cryoinjury (Fig. 1). Metal probe (cryoprobe) is cooled in liquid nitrogen and then ventricle is cauterized, causing massive necrosis of cardiac cells (20 % in area of injury) (Chablais *et al.*, 2011). Afterwards, clearance of necrotic cells by macrophages starts and fibrotic scar is formed. Next, as during resection cardiomyocytes dedifferentiate and start to proliferate. By 130 dpi scar is degraded and zebrafish heart is fully functional (González-Rosa *et al.*, 2011). This delay is probably caused by clearance of necrotic cells which together with fibronectin deposition recapitulates MI in mammals. However, stage of cardiomyocytes cell cycle entry is unique to *Danio rerio* (Jopling *et al.*, 2010; Kikuchi *et al.*, 2010).

Resection and cryoinjury heart regeneration models, both need invasive surgical procedure with mechanical injuries. Thus, cell-specific genetic ablation was established (Fig. 1). Procedure is based on inducible eradication of cardiomyocytes, where bacterial NTR or Diphtheria toxin A (DTA) chain is specifically expressed in myocardial cells. If harmless prodrug (Metronidazole) is injected into organism, nitroreductase catalyses its reduction into a cytotoxic compound causing cell death (Curado *et al.*, 2008). Wang and colleagues (2011) created the zebrafish´s transgenic line with 4- hydroxytamoxifen-inducible Cre-recombinase activity which is under the control of cardiomyocyte-specific myosin light chain 2 (cmlc2) promoter. This promoter launches the expression of DTA after injection of 4-hydroxytamoxifen. This leads to massive cardiomyocyte death (over 60 %) without any mechanical damage (Wang *et al.*, 2011).

For a heart regeneration experiments in rodents and larger animals, surgical ligation of left descending coronary artery is used. Ligation is cutting off blood flow and after 24 hours ischemic cell death appears. This technique best simulates MI as an ischemic area is created downstream to ligation and like cryoinjury it results in cell necrosis. Afterwards, fibronectin and collagen deposition start (Haubner *et al.*, 2012).

3.2.2 *Danio rerio´s* heart regeneration

Teleost fish *Danio rerio* (Zebrafish) has been extensively studied due to its external development, transparent larval stage, complete genome sequencing, low cost maintenance, and the robust regeneration capacity of lost body parts, such as the retina (Vihtelic & Hyde, 2000), the spinal cord (Becker *et al.*, 1997) and the heart (Poss *et al*., 2002). Regenerative mechanisms of different body parts in zebrafish seem

to be organ specific. As, typical epimorphic regeneration can be found after fin injury, where all stages including blastema formation occur (Chassot *et al.*, 2016). In contrast, spinal cord injury induces proliferation of neuron progenitor cells. New neuron cells are incorporated between undamaged cells, but natural cellular composition is not restored (Reimer *et al.*, 2008), as in case of fin regeneration.

Zebrafish has two-chambered heart, where the first and definitive sign of complete regeneration was interpreted in a work of Poss *et al.* (2002). They used histological technique to show, that after 2 months after partial ventricular resection (20 %), complete cardiac regeneration occurred. Where few seconds after surgical resection of apex, massive bleeding was stopped by immediate blood coagulation and blood clot formation. After reaching 2- 4 days post amputation (dpa), fibronectin started to incorporate into blood clot, reaching its maximum deposition levels at 7 dpa. By 30 dpa almost all residual fibronectin tissue was replaced by cardiomyocytes. Complete regeneration of a resected apex occurred at 60 dpa (Poss *et al.*, 2002; Chablais & Jaźwińska, 2012). Cardiomyocyte´s regeneration similarly to spinal cells, do not exhibit blastema formation. But rather undergo proliferation and partial dedifferentiation of the residual cardiac cells as shown during experiments of genetic fate-mapping (Jopling *et al.*, 2010). Next, Kikuchi *et al.* (2010) confirmed, that cells which contribute in regeneration are proliferating cardiomyocytes (no stem cells) and they can be tracked after injury, by embryonal gene reactivation *Gata4* (Zeisberg *et al.*, 2005).

3.2.3 *Xenopus´s* heart regeneration

Like Zebrafish, *Xenopus* also exhibits external development and transparent larval stage. Embryos are easily accessible for genetic manipulation or microinjection assays. They display extraordinary regenerative capacity of a lost tissue. However, compared to Zebrafish, they undergo metamorphosis and afterwards become juvenile and adults. After metamorphosis all anurans lose regenerative capacity, due to immune system maturation and cellular differentiation.

However, current approach in cardiac regeneration studies are focused mainly on zebrafish and mice. As previously mentioned, zebrafish possess a high capacity of heart regeneration (Poss *et al.,* 2002), while adult mice as a mammalian model lacks this ability (Jesty *et al.*, 2012). On the other hand, experimental evidence of cardiac regeneration

capacity in anurans was lacking until latest research from Liao *et al.* (2017) and Marshall *et al*. (2017, 2019). Years before these researches, Rumyantsev (1973) observed partial cardiac repair, after the ventricle crushing in *Rana temporaria*. However, as shown in this study, no complete regeneration, but rather cell cycle re-entry, DNA synthesis, and partial dedifferentiation occurs, without complete cardiac repair (Rumyantsev, 1973). Thus, until now, knowledge about capacity to regenerate lost cardiac tissue in anurans remained unclear. However, *Xenopus* model is frequently used for regeneration studies of limbs and tail. Here, *Xenopus* displays complete epimorphic limb regeneration in stage 50 after removing part of hind limb. In this stage regenerated limb is completely functional. When *Xenopus* embryos undergo metamorphosis, their limb regeneration capacity is lost (Satoh *et al.*, 2005). The main difference between embryo and adult is in immune system maturation, and as consequence even different inflammatory responses. Tadpoles mainly overcome inflammatory response after injury and are capable to regenerate. On the other hand, adult´s mature immune system displays complex immune response to injury and results rather in fibric spike, than in functional limb formation (Fukazawa *et al.*, 2009).

Marshall and colleagues (2017) partially fullfill knowledge gap of cardiac regeneration in *Xenopus* as they demonstrated expected results on adult (5 years old) *X. laevis,* as this model orgnism was not able to regenerate cardiac muslce after apical resection. Their analysis confirmed similar adult´s heart immune response after injury as in limb regeneration. Where heart displayed noticable early inflamation, followed by overexpression of fibronectin genes *col1a1*, *fn1* and hypertrophy gene *odc*. Fibronectin depostion early accumulated in injury site, but became most invasive at 1 month post amputation. When compared to zebrafish in this stage of regeneration, almost all residual fibronectin was replaced by newly formed cardiomyocytes (Poss *et al.*, 2002). Furthermore, Marshall´s group next analysed cardiac regeneration also in tadpoles. This study confirmed that tadpoles before metamorphosis are able to regenerate cardiac damage caused by resection. But more interestingly that animal loses its regeneration capacity as metamorphosis progresses. When injury is performed in prometamorphic stage 57-58, complete regenerative capacity is decreased over 45 % and in metamorphic stage 65-66 over 70 % (Marshall *et al.*, 2019).

In contrast with adult *X. laevis*, *X. tropicalis* surprisingly displayed complete cardiac regeneration after apical resection as described in work of Liao *et al.* (2017). They reported that the heart structure of *X. tropicalis* could be rebuilt within 30 dpa but with variations

in minimal scar deposition. For analysis, phospho-histone H3 (PH3) and anti-alpha skeletal muscle actin (α-SA) primary antibodies were used. PH3 positive cells, which indicated mitotic cardiomyocytes, were found in damaged area between 2-16 dpa. α-SA is marker for cardiomyocytes and in double-staining immunofluorescence experiment, Liao and colleagues found that PH3/α-SA positive cells were at peak level 16 dpa. At 30 dpa, levels of PH3/α- SA positive cells were significantly decreased, which accordingly to authors, indicated formation of newly matured cardiomyocytes (Liao *et al.*, 2017).

3.3 Molecular signalling and cellular pathways of cardiac regeneration

Molecular and signalling pathways of cardiac regeneration are assumed to be conserved among species. It is considered as a recapitulation of the developmental pathways in embryogenesis, with differences only in early events after injury (Jopling *et al.*, 2010). However, regulation of these pathways differs in non-regenerative and regenerative animals and tissues. One of the earliest events at the injury site is inflammation followed by elimination of the cellular debris. Further action consists of ECM deposition, which ensures ventricle wall stiffness at injury site, but for successful cardiac tissue remodelling, ECM has to be replaced by newly formed cardiomyocytes. If increased levels of ECM are not degraded, it can lead to alterations in ventricular function and heat failure (Lai *et al.*, 2017).

3.3.1 Inflammation signalling after cardiac injury

Inflammatory response at the injury site initiates tissue remodelling and its regulation is critical for regenerative process. Unlike embryonic development, where inflammation does not naturally occur, in regeneration it has crucial role in clearance of necrotic cells, survival of resident cells, tissue growth, and revascularization. Complex inflammatory response is composed of immune and mast cells accumulation, cytokines expression that modulate inflammation and ECM remodelling. Accurate regulation of inflammation is needed due to its favourable effects on regeneration and balance between

pro-inflammatory and anti-inflammatory responses is essential (reviewed in King *et al.*, 2012).

Activation of innate immune response aimed at an injury healing, is primary launched by danger-associated molecular patterns (DAMPs) released by necrotic cardiomyocytes. One of them is a pro-inflammatory cytokine high-mobility group box 1 (HMGB1), which is ligand for pattern recognition receptors, as the receptor for advanced glycation end products (RAGE) and Toll-like receptors (TLRs) (Herzog *et al.*, 2014). TLRs are evolutionary conserved transmembrane receptors, which activity can be modulated by expression on cell surface. They are able to regulate negative and positive feedback loop of innate immune response (Arslan *et al.*, 2010). Throughout binding of DAMPs to TLRs and recruitment of adaptor proteins such as myeloid-differentiation primary response protein 88 (MyD-88), nuclear factor kappa-light-chain-enhancer of activated B cells (NF-κB) is activated and it translocates to cell nucleus (Lugrin *et al.*, 2015). Here it initiates an expression of key pro-inflammatory cytokine, interleukin 6 (IL-6), but also anti-inflammatory interleukin 10 (IL-10) and tumor necrosis factor α (TNF-α) (Rao *et al.*, 2014). *In vivo* murine experiments performed by Lugrin and colleagues (2015), demonstrated that necrotic myocardial tissue releases interleukin 1α (IL-1α) after MI. On the other hand, inflammation in IL-1α$^{-/-}$ mice, was disrupted after MI (Lugrin *et al.*, 2015). The type 1 Interleukine-1 receptor (IL-1R1) is sufficient to mediate IL-1 signalling and it was demonstrated by Bujak and colleagues (2008), who examined effects of disrupted signalling with use of IL-1R1$^{-/-}$ mice after MI. Mice exhibited decrease not only in inflammatory response but also in fibronectin and collagen deposition, which are sufficient for injury closure and maintenance of structure. However, this downregulation has a potential for cardiac regeneration, because during normal inflammation, fibronectin and collagen deposition levels are excessive. High levels of fibronectin depositions then negatively affect heart function and it cannot be removed as in zebrafish heart after injury (Poss *et al.*, 2002). Other key step in innate immune response to cardiac injury is infiltration of neutrophils and macrophages, which was also reduced in this model (Bujak *et al.*, 2008). Another important inflammatory signalling is Smad3-dependent transforming growth factor β (TGFβ) pathway. Chablais and Jaźwińska (2012) illustrated, that TGFβ ligands were locally induced at injury site and expressed by infiltrated leukocytes and fibroblast-like cells.

Neutrophils and macrophages are attracted by such factors as DAMPs, chemokines, and cytokines released from dying cells and growth factors such as TGFβ, TNF-α, complement component 5a (C5a), IL-6, interleukin 8 (IL-8) and intercellular adhesion molecule 1 (ICAM-1) (Kukielka *et al.*, 1995). In the wound area, neutrophils are responsible for release of proteolytic enzymes, clearance of necrotic cells, ECM debris, and high levels production of reactive oxygen species (ROS). Secretome of neutrophils, contain also neutrophil gelatinase-associated lipocalin (NGAL), which is substantial for recruitment of another important cell component of immune response, macrophages (Horckmans *et al.*, 2017). Resting macrophages can differentiate into 2 phenotypes of M1 and M2, whereas M1 phenotype secrete pro-inflammatory cytokines, such as interleukin 12 (IL-12) while M2 macrophages are mainly anti- inflammatory with production of IL-10 (Edwards *et al.*, 2006). Importance of innate immune system response via macrophages was demonstrated by Godwin *et al.* (2017), who performed macrophages depletion after cardiac injury in adult salamander, which resulted in regeneration failure. However, salamander is normally capable of complete regeneration. Next, comparative transcriptomic analyses after cardiac injury in zebrafish and medaka described differences in monocytes/macrophages infiltration dynamics (Lai *et al.*, 2017). These organisms are phylogenetically closely related, but medaka fails to regenerate lost cardiomyocytes (Ito *et al.*, 2014). Lai and colleagues observed delayed and reduced macrophage recruitment in medaka after cryoinjury, compared to zebrafish. Next, they delayed recruitment of macrophages in zebrafish by injection of clodronate liposomes one day before injury. It resulted similarly to medaka, into scar formation and regeneration failure (Lai *et al.*, 2017).

Crucial role of acute inflammation suppression after cardiac damage in the heart regeneration was demonstrated by Wan *et al.,* (2013), where macrophage myeloid-epithelial-reproductive tyrosine kinase (MERTK) in mice´s phagocytes was sufficient for necrotic cell clearance. In $Mertk^{-/-}$ mouse IL-6 levels were significantly higher and IL-10 levels significantly lower compare to $Mertk^{+/+}$ mouse at 7 dpi. It leads to increase in infarct size, prolonged inflammation and reduction in the heart performance. Infiltrated lymphocytes in damaged heart express anti-inflammatory IL-10, which modulate healing process via JAK/STAT pathway, by induction of tissue inhibitor of metalloproteinases 1 (TIMP-1), a key modulator of matrix metalloproteinases (MMPs) activity. TIMP-1 favours in ECM deposition increase, which ensures maintaining heart structure after MI

(Riley *et al.*, 1999; Frangogiannis *et al.*, 2000). IL-10 simultaneously downregulate inflammatory response via inhibition of cytokines, such as TNF-α, IL-1α, IL-1β, and IL-6 (Riley *et al.*, 1999; reviewed in Wojdasiewicz *et al.*, 2014).

All these data suggest that response of innate immune system is needed for successful heart regeneration. However, its regulation is necessary and pro-inflammatory reaction has to be downregulated during/after necrotic cells clearance. If necrotic cells are not cleared and pro-inflammatory response is prolonged, or there is inaccuracy in cytokine signalling, it results in regeneration failure and adverse tissue remodelling.

3.3.2 ECM signalling and deposition

In embryonic development ECM provides paracrine signalling, which results in cardiomyocyte proliferation and differentiation. One of the key signalling components of ECM are fibroblasts, which produce MMPs, integrins and proteins such as fibronectin, collagen, laminin, osteopontin, tenascin, periostin, and growth factor like a heparin-binding epidermal growth factor (EGF)-like growth factor (Ieda *et al.*, 2009; Mosqueira *et al.*, 2014).

Similarly, regenerative response to cardiac injury, results in ECM and tissue remodelling. In neonatal mouse, with minimal scar formation, which is nevertheless degraded and replaced by newly formed cardiomyocytes, compared to adult mammals (Porrello *et al.*, 2011). Garcia-Puig *et al.* (2019) with liquid chromatography–mass spectrometry (LC-MS) analysis demonstrated, that in zebrafish´s heart, fibronectin 1b (fn 1b), periostin 1b (postnb), collagen 4 (col 4) and collagen 5 (col 5) reached peak levels at 7 day post injury. Further, at 30 dpi all of them were degraded at levels of control hearts without injury.

Cardiac fibroblasts also react to stress with production of factors as TNF-α, IL-1β, fibroblast growth factor 2 (FGF 2), endothelin-1 (ET-1) and TGFβ ligands (Chablais and Jaźwińska, 2012; reviewed in Manabe *et al.*, 2002), which leads to fibrosis. TGFβ pathway was mentioned in inflammatory response, on the other hand it also influences reparative remodelling via ECM deposition. When necrotic cells are cleared at 4 dpi, infiltrated fibroblast-like cells are stimulated to produce collagen-rich ECM via TGFβ/Activin signalling. However, this signalling has an even wider application. It is responsible for re-activation of cardiomyocytes and its proliferation via Tenascin C upregulation. Tenascin C is ECM protein, which is upregulated under

pathological conditions (Chablais & Jaźwińska, 2012). MMPs together with TGFβ play an important role in ECM turnover. It has been shown, that activity of MMP 2 increases with collagen 1 (col 1) synthesis, which is regulated by TGFβ signalling. Stawowy *et al*. (2004) demonstrated, that MMP2 expression via TGFβ signalling, promotes migration of cardiac fibroblasts, which induces ECM proteins production and fibrosis formation. As previously shown, TIMPs are main inhibitors of MMPs and the balance between degradative enzymes and their inhibitors is what ensures ECM remodelling and proper healing. Any deviation in regulatory pathways causes pathological scar formation (Uchinaka *et al.*, 2014).

3.3.3 Cardiomyocyte proliferation and differentiation signalling

After remodelling processes, all residual ECM is degraded and substituted with newly formed cardiomyocytes. Hypotheses about new cardiomyocytes source are still under debate, but two most discussed variants are, that cells which contribute on new cardiomyocyte formation are from non-damaged pre-existing cardiomyocytes, which undergo dedifferentiation and cell cycle re-entry. The second hypothesis operates with existence of cardiac progenitor cells (CPCs) or cardiac stem cells (CSCs), which respond to injury by differentiation into cardiomyocytes (Senyo *et al.*, 2013; Li *et al.*, 2018). In mammals, an isotope genetic-fate mapping revealed that damaged myocardial cells are replaced by low rates of pre-existing source of cardiomyocytes during postnatal live and cardiomyogenesis occurs only in limited rates by the division (Senyo *et al.*, 2013). However, in neonatal mouse, main source of newly formed cardiomyocytes are stem cells (Li *et al.*, 2018), and within 7 days after birth can fully regenerate its lost cardiac tissue (Porrello *et al.*, 2011). On the other hand, adult hearts of lower vertebrates (zebrafish) display high plasticity and as a reaction to injury are able to trigger dedifferentiation and proliferation of cardiac cells (Jopling *et al.*, 2010). Epigenetic reprograming is one of the key factors for molecular regulation of cardiac regeneration, which downregulate cardiac structure and function genes (for example: myosin light chain kinase 3 (*Mylk3*), myopalladin (*Mypn*), cardiac Troponin T (*TnnT*) and Titin (*Ttn*)) while genes for cell cycle and proliferation (for example: cyclin D2 (*Ccnd2*), cyclin-dependent kinase 4 (*Cdk4*) are upregulated (Zhang *et al.*, 2015a).

Understanding of molecular regulation of cardiomyocyte cell cycle re-entry and proliferation in animals with regenerative capacity is potential therapeutic target for cardiac regeneration in adult mammals. Hippo signalling pathway controls organ size development in embryo. Its regulation was also demonstrated in mice heart development by Heallen and colleagues (2011) in Hippo-deficient mouse, which developed overgrown hearts with robust cardiomyocyte proliferation and increased WNT/β-catenin signalling. Further, same group performed regeneration experiments in a same model and these experiments showed expected results, when Hippo-deficient adult mouse after MI, enhanced survival and proliferation of cardiac cells and recovered heart function to control hearts without knockout and MI (Heallen *et al.*, 2013). Hippo effector Yes-associated protein (Yap) is a key transcription factor for apoptotic and proliferative genes expression. Its depletion in neonatal mouse resulted in extensive fibrotic scarring after coronary ligation compared to control mice, which effectively regenerated lost cardiac tissue. On the other hand, constitutively activated Yap in adult mouse resulted in improved survival of cardiomyocytes after MI, enhanced proliferation and cardiac regeneration with almost no fibrosis. Activated Yap stimulates insiln-like growth factor (IGF), which launches a phosphorylation of protein kinase B (Akt) and inhibition of GSK-3, a key factor for regulation of WNT/β-catenin signalling (Xin *et al.*, 2013).

Another transcription factor important for cardiac development is GATA4. It has been demonstrated that, GATA4 is downregulated in neonatal mouse at 7 day after birth. However, during 6 days after birth GATA4 is strongly expressed and mice is capable of heart regeneration. Cardiomyocyte-specific knockout of GATA4 disrupts heart regeneration in mice at 1 day after birth. Furthermore, its overexpression by adenoviral gene transfer in wild-type mice boost recovery of cardiac tissue at first day of postnatal life (Mohammadi *et al*., 2017).

Growth factors like fibroblast growth factor 1 (FGF 1) play also important role in the heart repair. In cardiac regeneration they are locally released at injury site. Here, it binds to receptors and regulates cell survival, wound healing, angiogenesis, and mitotic activity. FGF 1 promotes dedifferentiation of cardiomyocyte and cell cycle re-entry. However, cell cycle can be suppressed by p38 mitogen-activated protein kinases (p38 MAPK) in G2/M checkpoint control. Inhibition of p38 MAPK together with FGF1 injection in adult rats after MI promoted cardiac regeneration, and showed higher levels of Cyclin D2, and Cyclin A compared to controls (Engel *et al.*, 2005, 2006).

Molecular and cellular signalling after cardiac injury in animals with regenerative capacity is very accurately regulated. If any error appears, cardiac regeneration is disrupted. However, understanding of these pathways and its regulation are promising ways for launching cardiac regeneration therapy in adult mammals.

3.4 MSCs therapy in the heart regeneration

MSCs are connective (stromal) tissue cells with multipotent differentiation capacity into various tissues of mesoderm. They are mainly derived from bone marrow or adipose tissue (Abdi *et al.*, 2008). Characteristic features of these cell types are, adherence to plastic surface, formation of fibroblast-like shape, formation of colonies and differentiation into 3 cell lineages: adipocytes, chondrocytes and osteocytes. Typical MSCs also express key markers as CD73, CD90, and CD105, but need to be absent for CD11b, CD14, CD19, CD34, CD45 and human leukocyte antigen-DR (HLA-DR) (Dominici *et al.*, 2006). Due to, its biological properties, such as differentiation potential, anti-inflammatory properties, immunomodulation and neuroprotection, MSCs are nowadays used in clinical trials (Sahraian *et al.*, 2019). Intravenous injection delivery of MSCs is one of possible treatment for tissue repair, where it was predicted differentiative effect into damaged cells. However, intravenous grafts of MSCs resulted in high death rates of MSCs, decrease in coronary blood flow and most of them were captured in lungs (Freyman *et al.*, 2006; Toma *et al.*, 2009). Further, *in vivo* differentiation of MSCs into targeted cells occurs only in low rates. Nevertheless, survived cells after engraftment start to produce immunomodulatory factors, which influence tissue repair more than differentiation alone (Katsha *et al.*, 2011). Another approach in MI therapy focused on injection of MSCs into skeletal muscle. It is a noninvasive strategy and it was demonstrated, that MSCs in muscle bed positively influence heart function and regeneration within 1 month after injury (Shabbir *et al.*, 2009). This led to change in MSCs therapy approach, into secretome control by paracrine and growth factors. High levels of pro-inflammatory cytokines, such as IL-1α, IL-1β, TNF-α, and interferon gamma (IFNγ) activate MSCs and launch expression of chemokines and inducible nitric oxide synthase (iNOS) (Ren *et al.*, 2008). Secretome of MSCs also includes TGFβ, hepatocyte growth factor (HGF), stromal cell derived factor-1 (SDF-1), IL-6, prostaglandin E2 (PGE_2), and indoleamine 2,3-dioxygenase (IDO) (Bai *et al*., 2012; Bouffi *et al*., 2010; Hung *et al*., 2013; Landry *et al.*, 2010; Meisel *et al*., 2004; Ylostalo *et al*.,

2012). MSCs secretome influences inflammatory reaction of neutrophils, macrophages, natural killer cells, mast cells and dendritic cells. For instance, PGE2 can modulate macrophages into anti-inflammatory phenotype M2, with a high production of IL-10, but also induce immunomodulatory regulatory T-cells (Baratelli *et al.*, 2005; Németh *et al.*, 2009). Thus, injection of MSCs and its paracrine effect boost cardiac regeneration, modulate immune response, improve angiogenesis, increase survival of cardiomyocytes, and improve cardiac function after MI (Timmers *et al.*, 2011; Zhao *et al.*, 2016).

3.5 Sertoli cells: immunomodulatory guards of testicles

Testicles consist of seminiferous tubules surrounded by interstitial tissue and peritubular myoid cells. Another cell type are Sertoli cells, which provide nourishing of developing sperm cells, within seminiferous tubules (Fig. 2) (Dym & Fawcett, 1970). In development, Sertoli cells provide signalling via anti-Müllerian hormone (AMH), which contribute to female Müllerian duct regression (Taguchi *et al.*, 1984). Sertoli cells in adult testes contribute to phagocytosis of apoptotic spermatocytes, control environment of seminiferous tubules and secrete paracrine factors involved in germ cell maturation. Testis are immune-privileged organ, because germ cells express novel antigens and intracellular proteins that can be recognized by immune system and evoke auto-immune response. It was demonstrated also on skin graft experiments into testes, where transplanted cells survived long period of time and did not launch immune response (Head *et al.*, 1983). In order to protect germ cells from immune response, Sertoli cells form blood-testis barrier (BTB) and produce immunomodulatory factors. BTB is composed of neighbouring Sertoli cells connected with tight and gap junctions (Fig. 2) (Dym & Fawcett, 1970). Immunomodulatory paracrine factors secreted by Sertoli cells are for example TGFβ, IDO, galectin 1, activin A. All these factors regulate immune cells that way, they suppress pro-inflammatory reactions and shift them into anti-inflammatory and peripheral tolerance manner (Wollina *et al.*, 1999; O'Bryan *et al.*, 2005; Fallarino *et al.*, 2009). Immunomodulatory properties of Sertoli cells were demonstrated by Fallarino and colleagues (2009), who performed xenograft experiment of pig´s immature Sertoli cells into peritoneal cavity of diabetic mouse. Sertoli cells alone without any co-transplanted cells,

recovered diabetes type 1 in nonobese diabetic mouse and increased levels of regulatory T cells.

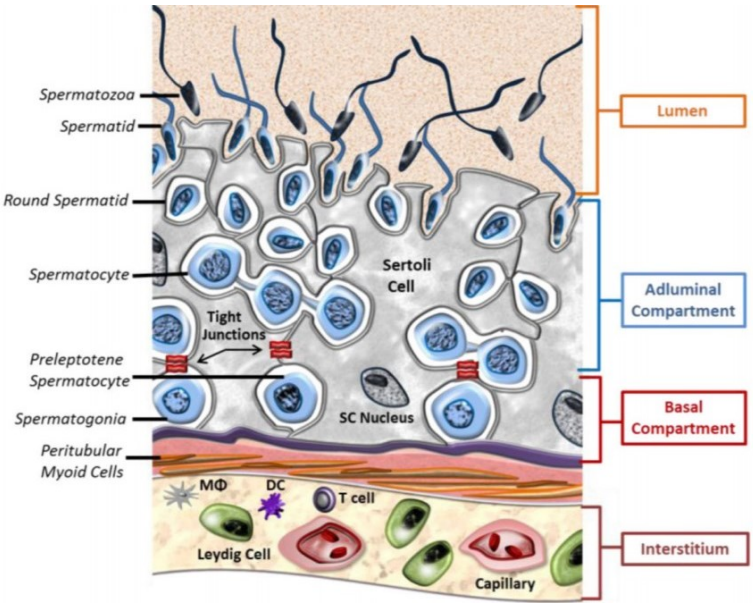

Figure 2. Illustration of cross-section of seminiferous tubule and BTB barrier in testicles: Testicles consist of interstitum and seminiferous tubules, which are divide into basal and adluminal compartments and lumen. Macrophages (MΦ), Dendritic cells, T cells, Leydig cells and capillary network are localized in interstitium. Sertoli cells, germ cells and peritubular myoid cells form seminiferous tubules. Neighbouring Sertoli cells connected via tight junction create immunological barrier (BTB), which create from testicles immune privileged organ of body (adopted from Kaur *et al.*, 2014).

3.5.1 *Xenopus tropicalis* immature Sertoli cells (XtiSCs)

Our laboratory of developmental biology successfully established immature Sertoli cell line of XtiSCs. These cells were isolated from *X. tropicalis* juvenile (6-months old) testes. Afterwards, Katushka red fluorescent protein (RFP) under CAG promotor was inserted into genome of XtiSCs. Reverse transcription polymerase chain reaction (RT- PCR) analysis detected pluripotency marker kruppel-like factor 4 (*klf4*), telomerase reverse transcriptase (*tert*), and *c-myc.* However, expression of other pluripotency markers, such as octamer-binding transcription factor 4 (*oct4*) and sex determining region Y box 2 (*sox2*), were reduced. On the other hand, not germ but somatic cell origin was confirmed by expression inhibition of *dazl*, *ddx4* and *ddx25*, the germ cell markers. Another analysis revealed expression of vimentin, cytokeratin and some MSCs markers, which confirms immature Sertoli cells phenotype (Tlapakova *et al.*, 2016).

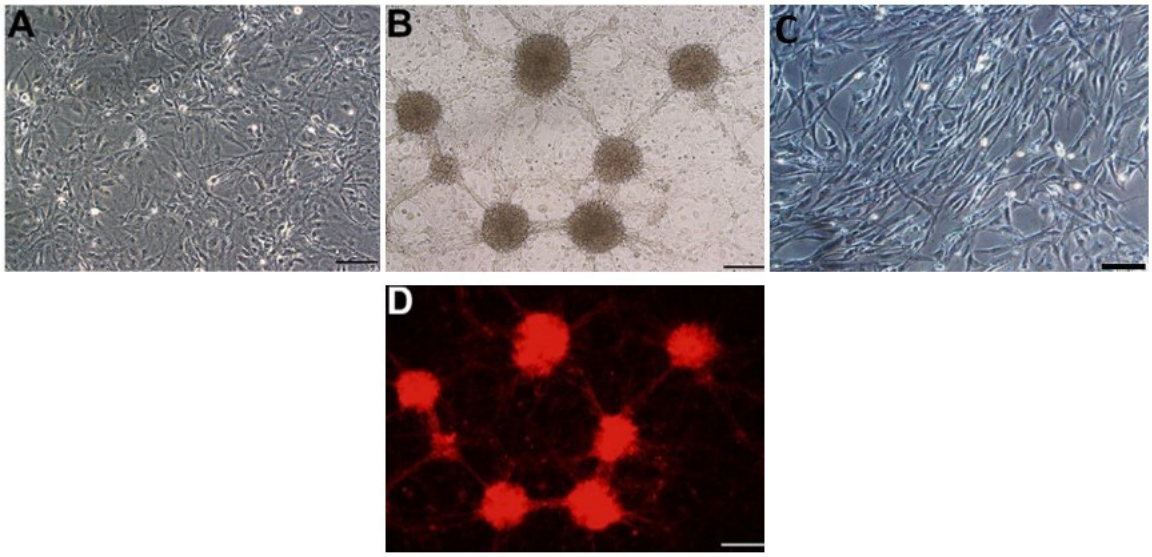

Figure 3. XtiSCs cell culture characterization:
(A) XtiSCs cell culture in monolayer and short term cultivation, **(B)** Formation of cell colonies in long term cultivation of XtiSCs, **(C)** XtiSCs after 3 day treatment with GSK-3 inhibitor CHIR 99021, notable morphological changes into fibroblast-like shape, **(D)** RFP-positive cell colonies of XtiSCs Scale bar A,C: 100 µm; scale bar B,D: 200 µm (adopted from Nguyen *et al.*, 2019; Tlapakova *et al*., 2016)

Within cultivation, XtiSCs adhere to plastic surface of cultivation bottle, forms colonies in long term cultivation. After treatment with pharmacological inhibitor of GSK-3 (CHIR99021), XtiSCs form fibroblast-like shape (Fig. 3). At 3 days of CHIR99021 treatment XtiSCs mimics phenotype of MSCs-like cells and are able to differentiate into adipocytes, chondrocytes and osteocytes (Nguyen *et al.*, 2019). Transplantation experiments of XtiSCs into *X. tropicalis* embryo at stage 51, demonstrated migratory effect to wound area and differentiation potential into cardiomyocytes (Fig. 4) (Nguyen, 2019). All these data suggest, that XtiSCs have all the characteristic features of immature Sertoli cells with possible immunomodulatory paracrine effects of Sertoli cells. But also, after treatment with GSK-3 inhibitor CHIR99021 could have limited differentiation properties of MSCs (Nguyen, 2019).

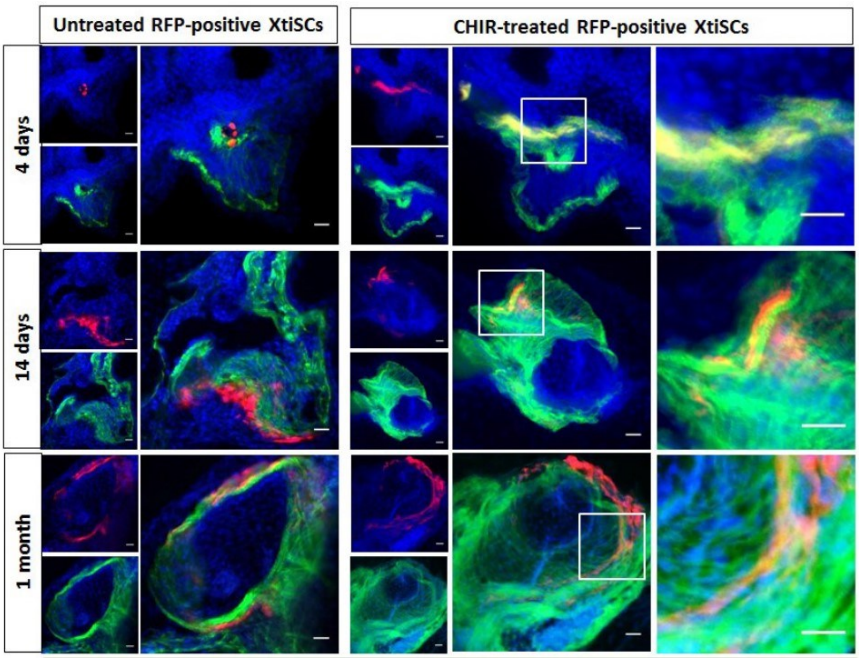

Figure 4. Differentiation of CHIR99021 treated XtiSCs into cardiomyocytes *in vivo*:
XtiSCs differentiation at 4th, 14th and 1-month post microinjection into peritoneum of tadpole. Green- cardiac troponin T, red- XtiSCs, blue- nuclei, yellow- colocalization of red and green fluorescent signal, which represent differentiation of XtiSCs into cardiomyocytes. Scale bar: 20 µm. (adopted from Nguyen, 2019)

4 AIMS OF THESIS

- Standardization of XtiSCs-RFP microinjection protocol regarding stage 50+ tadpole´s heart.
- Standardization of apical resection (surgery) protocol of adult *X. tropicalis* heart.
- Study of colonization and proliferation of XtiSCs-RFP treated with CHIR99021 in tadpole´s (stage 50+) and adult´s *X. tropicalis* heart.
- Study of the effect of transplanted XtiSCs-RFP (with/without CHIR 99021 treatment) on fibrotic scar formation after heart injury in adult *X. tropicalis*.
- Standardization of methods for sample sectioning and its analysis.

5 MATERIAL

5.1 Chemicals

Title of chemical/media	Supplier
β-mercaptoethanol (55mM)	Life Technology
Acetic acid (glacial)	Penta
Agarose	Lonza
Aniline blue	Lachema
Benzene	Penta
Blocking reagent	Boehringer Mannheim GmbH
Bovine serum albumin	Sigma-Aldrich
CHIR99021	Sigma-Aldrich
Chromium potassium sulphate dodecylhydrate	Lachema
Cysteine	Sigma-Aldrich
EGTA	Sigma-Aldrich
Entellan	Euromex
Eosin	Lachema
Ethanol (96%)	Penta
Ethanol (absolute)	Penta
Foetal bovine serum	Sigma-Aldrich
Formaldehyde (37%)	Penta
Fuchsin (acidic)	Lachema
Gelatine	Emprove
Gentamicin (50µl/mL)	Sigma-Aldrich
Gentamicin – GENTAVETo (50µl/mL)	V.M.D. n.v./s.a.
Gill´s hematoxylin	Carl Roth
HEPES	Life Technologies
Human chronic gonadotropin hormone (C1063)	Sigma-Aldrich
L-15 medium Leibovitz	Life Technologies
L-glutamine (200mM)	Sigma-Aldrich
Low melting agarose	Carl Roth
Magnesium dichloride	Lachema
Magnesium sulphate	Lachema
Methanol (100%)	Penta
MOPS	Sigma-Aldrich
Mowiol/DAPI	Sigma-Aldrich
O.C.T.™Compound 4583	Tissue-Tek
Papain (61,25 µg/ml)	Biochrom AG
Paraffin oil	Carl Roth
Paraffin Paraplast plus	McCormick Scientific
Paraformaldehyde	Sigma-Aldrich
Phosphomolybdic acid	Sigma-Aldrich
Picric acid (saturated)	Sigma-Aldrich
Ponceau	Lachema
Potassium dihydrogen phosphate	Lachema
Potassium chloride	Lachema
RPMI 1640 medium	Life Technologies
Saccharose	Penta

Sodium dodecyl sulphate	Sigma-Aldrich
Sodium hydrogen carbonate	Sigma-Aldrich
Sodium chloride	Penta
Sodium phosphate dibasic dihydrate	Lachema
Sodium pyruvate (100mM)	Sigma-Aldrich
Tricaine Methanesulfonate (MS222)	Sigma-Aldrich
TRIS hydrochloride	Sigma-Aldrich
Tri-sodium citrate (dihydrate)	Sigma-Aldrich
Triton X-100	Sigma-Aldrich
Trypsin-EDTA	Biosera
Tween 20	Sigma-Aldrich
Weigert´s hematoxylin	Carl Roth
Xylene	Penta

5.2 Instruments

Title of instrument	Supplier
Centrifuge Hettich Universal 32 R	Hettich Zentrifugen
Countess® Automated Cell Counter	Invitrogen
Cryotome CM3050 S	Leica
Flow box EM Box 120	Scholler Instruments
Fluorescence microscope Olympus BX40	Olympus Optical
Fluorescence stereomicroscope Olympus SZX16	Olympus Optical
Heating plate VD-1	Vezas
Hybridization oven HO-10	Stovall Life Science
Inversed microscope Olympus BX40F	Olympus Optical
MCO-19 AIC Sterisonic UVH Incubator	Panasonic
Microinjector IM 400 with sucking module IM 400B	Narishige
Micropipette puller PC-10	Narishige
Microtome HM 310	Microm
Microtome RM2255	Leica
Stereomicroscope Stemi 2000	Zeiss
Vibratome VT 1200 S	Leica
Vortex Ika Works Minishaker MS1	Ika Works
Water bath Techne TE 10D Tempette	Techne

5.3 Other material

Title of material	Supplier
2-0 multifilament silk suture with cutting needle	Ethicon
Glass capillary for microinjection	Drummond
Insulin syringe & needle 27g x 0.5" x 100 (0.5mL)	Terumo
Microscope slides	P-Lab
Microscope Super Frost Plus slide (white)	Thermo Fisher Scientific
Pap pen	Kisker
Petri dish	P-Lab

Razors	Astra
Sterile cotton	Hartmann
Strainers Cell Trics® 20 µm	Partec
Surgical table for small animals	Own production

5.4 Primary antibodies

Cat./Clone. No	Antigen	Species	Supplier	Dilution
CH1	Cardiac Tropomyosin	Mouse	Developmental Studies Hybridoma Bank	2 µg/ml
CT3	Cardiac troponinT	Mouse	Developmental Studies Hybridoma Bank	2 µg/ml
AB233	Red fluorescence	Rabbit	Evrogen	1:5000
F 3648	Fibronectin	Rabbit	Sigma-Aldrich	1:500

5.5 Secondary antibodies

Cat./Clone No.	Antigen	Species	Supplier	Dilution
A11001	Mouse IgG- Alexa Fluor® 488 conjugate	Goat	Thermo Fisher Scientific	1:500
A11012	Rabbit IgG- Alexa Fluor® 594 conjugate	Goat	Thermo Fisher Scientific	1:500

5.6 Animals

Experiments involved adult *X. tropicalis* (Nigerian strain, 4 years old, Nosek, 8 years old) and tadpoles (stage 50+). Animals were housed in a facility with light:dark (12:12 hours) cycles at 24-26 °C, in dechlorinated and filtered water with addition of sea salt (2.5 g/10 L). Daily feeding on commercial diet (Tetra).

5.7 XtiSCs culture

XtiSCs is a cell culture of immature Sertoli cells, which was established from testes of juvenile (6 months old) *X. tropicalis* (male, Ivory Coast) (Tlapakova *et al.*, 2016). Katushka red fluorescent protein (RFP) under CAG promotor was inserted into genome of XtiSCs. However, insertion of RFP is not homogenous in whole cell line, so to obtain cells with highest intensity of RFP signal, cells were sorted on fluorescence-activated cell sorter (FACS).

5.8 Solutions

5.8.1 Phosphate buffered saline

- *10x Phosphate buffered saline (PBS) (pH=7.4) (stock solution)*
  - 79 g NaCl
  - 29 g Na2HPO4.12H2O
  - 3.1 g KH_2PO_4
  - 1.1 g KCl
  - Volume adjusted to 1000 ml with distilled H_2O.

- *1x PBS (pH=7.4)*
  - 50 ml 10x PBS
  - Volume adjusted to 500 ml with distilled H_2O.

- *2/3 PBS (pH=7.4)*
  - 334 ml 1x PBS
  - Volume adjusted to 500 ml with distilled H_2O.

  **Xenopus* cells have different osmolarity (100mM) than mammalian cells (150mM). Thus, all solutions with salts concentration have to be diluted (2/3).

5.8.2 Fixation solutions

- *3.7% Formaldehyde*
  - 10 ml Formaldehyde (37%)
  - Volume adjusted to 100 ml with distilled H_2O.

- *10x MOPS + EGTA + Magnesium sulphate + Formaldehyde buffer (MEMFA) (pH=8) (stock solution)*
    - 20.93 g MOPS (1M)
    - 7.61 g EGTA (20mM)
    - 2.47 g $MgSO_4$ (10mM)
    - Volume adjusted to 100 ml with distilled H_2O.

- *1x MEMFA + 3.7% Formaldehyde*
    - 10 ml 10x MEMFA
    - 10 ml Formaldehyde (37%)
    - Volume adjusted to 100 ml with distilled H_2O.

- *4% Paraformaldehyde (pH=7.4)*
    - 4 g Paraformaldehyde
    - Volume adjusted to 100 ml with distilled H_2O.

  *This solution has to be heated in water bath for 1.5 hour. Afterwards 3 drops of 10M NaOH are added and afterwards paraformaldehyde will dissolve.

5.8.3 Medium for cell culture cultivation

- *Xenopus testicular cell 2/3 cultivation medium*
    - 150 ml L-15 Leibovitz
    - 30 ml 5x RPMI 1640
    - 45 ml Foetal bovine serum (FBS)
    - 4.5 ml L-glutamine (200mM)
    - 8 mL $NaHCO_3$ (7.5%)
    - 450 µl Gentamicin
    - 3 ml Sodium pyruvate (100 mM)
    - 818 µl β-mercaptoethanol
    - Volume adjusted to 450 ml with deionized H_2O.

5.8.4 In vitro fertilization (IVF) solutions

- *20x Marc's Modified Ringer's Solution (MMR) (pH=7.5)*
    - 58.44 g NaCl
    - 1.49 g KCl
    - 2.03 g $MgCl_2$
    - 11.92g HEPES (1M)
    - Volume adjusted to 500 ml with deionized H_2O.

- *0.05x MMR (pH=7.7)*
  - 2.5 ml 20x MMR
  - Volume adjusted to 1000 ml with deionized H_2O.

- *0.05x MMR + Gentamycin (pH=7.7)*
  - 2.5 ml 20x MMR
  - 1.0 ml Gentamycin (50 mg/ml)
  - Volume adjusted to 1000 ml with deionized H_2O.

- *1x MMR + Gentamycin (pH=7.7)*
  - 5 ml 20x MMR
  - 100 µl Gentamycin (50 mg/ml)
  - Volume adjusted to 100 ml with deionized H_2O.

- *2.2% Cysteine + 0,1x MMR (pH=7.7)*
  - 500 µl 20x MMR
  - 2.2g L-Cysteine
  - Volume adjusted to 100 ml with ddH_2O.

- *L-15 Leibovitz + 10% FBS medium*
  - 10 g Foetal bovine serum
  - Volume adjusted to 100 ml with L-15 Leibovitz.

- *0.4% MS222 (pH=7)*
  - 4 g MS222 (Sigma)
  - 4 g $NaHCO_3$
  - Volume adjusted to 1000 ml with ddH_2O.

- *1% Agarose (for Petri dish coating)*
  - 1 g agarose
  - Volume adjusted to 100 ml with 0.05x MMR.

5.8.5 Microinjection solution

- *0,2% MS222 (Sleeping solution)*
  - 0,2 g MS222
  - 0,2 g $NaHCO_3$
  - Volume adjusted to 100 ml with distilled H_2O.

5.8.6 Surgery (apical resection) solution

- *MS222 (800 mg/L)*
  - 800 mg MS222
  - 800 mg $NaHCO_3$
  - Volume adjusted to 1000 ml with distilled H_2O.

5.8.7 Killing solution

- *0,4% MS222 (killing solution)*
  - 0,4 g MS222
  - 0,4 g $NaHCO_3$
  - Volume adjusted to 100 ml with distilled H_2O.

5.8.8 Vibratome solution

- *4% Low Melting Agarose in 1x PBS*
  - 0.4 g Low Melting Agarose
  - Volume adjusted to 10 ml with 1x PBS.

5.8.9 Microtome solution

- *1:1 Benzene: Paraffin*
  - 20 ml Benzene
  - 20 ml Paraffin

5.8.10 Cryotome solutions

- *5% Saccharose in 2/3 PBS*
  - 5 g Saccharose
  - Volume adjusted to 100 ml with 2/3 PBS.

- *10% Saccharose in 2/3 PBS*
  - 10 g Saccharose
  - Volume adjusted to 100 ml with 2/3 PBS.

- *15% Saccharose in 2/3 PBS*
  - 15 g Saccharose
  - Volume adjusted to 100 ml with 2/3 PBS.

- *20% Saccharose in 2/3 PBS*
    - 20 g Saccharose
    - Volume adjusted to 100 ml with 2/3 PBS.

5.8.11 Solutions for slide coating for histological tissue sections

- *Gutenby´s glue*
    - 20 ml Ethanol (96%)
    - 6 ml CH_3COOH
    - 1.5 g Gelatine
    - 0.1 g $Cr_2 (SO_4)_3 K_2SO_4 \times 12H_2O$
    - Volume adjusted to 100 ml with distilled H_2O.

- *Gelatine glue*
    - 0,5 g Gelatine
    - 0.05g $Cr_2 (SO_4)_3 K_2SO_4 \times 12H_2O$
    - Volume adjusted to 100 ml with distilled H_2O.

5.8.12 Antigen retrieval solutions

- *Sodium citrate buffer (10 mM Sodium Citrate, pH=6)*
    - 2.94 g Tri-sodium citrate (dihydrate)
    - 500 µl Tween 20
    - Volume adjusted to 1000 ml with distilled H_2O.

- *TE buffer (10 mM Tris-Base,1 mM EDTA, pH=9)*
    - 1.21 g Tris-Base
    - 0.37 g EDTA
    - 500 µl Tween 20
    - Volume adjusted to 1000 ml with distilled H_2O.

- *PBS buffer (pH=7.5)*
    - 500 ml 1x PBS
    - 500 µl Tween 20
    - Volume adjusted to 1000 ml with distilled H_2O.

5.8.13 Blocking solutions

- *Tris-NaCl-Blocking buffer (TNB)*
  - 1.21 ml Tris-HCl (1M)
  - 0.88 g NaCl
  - 0.5 g Blocking reagent
  - Volume adjusted to 100 ml with distilled H_2O.

- *2% Bovine serum albumin (BSA) in 2/3 PBS*
  - 2 g BSA
  - Volume adjusted to 100 ml with 2/3 PBS.

5.8.14 Antifading solution

- *Cu_2SO_4 (5mM) in ammonia acetate (50mM) (pH=5.1)*
  - 0.11 g Cu_2SO_4
  - 0.38 g Ammonium acetate
  - Volume adjusted to 100 ml with 1x PBS.

5.8.15 Histological staining solutions

- *Eosin (stock solution)*
  - 2 g Eosin
  - 160 ml Ethanol (96%)
  - Volume adjusted to 200 ml with distilled H_2O.

- *Eosin*
  - 20 ml Eosin (stock solution)
  - 60 ml Ethanol (80%)
  - 0.4 ml CH_3COOH

- *Ponceau (stock solution)*
  - 1 g Ponceau
  - 1 ml CH_3COOH
  - Volume adjusted to 100 ml with distilled H_2O.

- *Fuchsin (acidic) (stock solution)*
  - 1 g Fuchsin (acidic)
  - 1 ml CH_3COOH
  - Volume adjusted to 100 ml with distilled H_2O.

- *Ponceau – Fuchsin*
    - 60 ml Ponceau (stock solution)
    - 30 ml Fuchsin (stock solution)

- *Aniline blue*
    - 2.5 g Aniline blue
    - 2.5 ml CH_3COOH
    - Volume adjusted to 100 ml with distilled H_2O.

- *1% HCl in 80% Ethanol*
    - 1 ml HCl
    - 83 ml Ethanol (96%)
    - Volume adjusted to 100 ml with distilled H_2O.

- *Bouin´s solution*
    - 75 ml Picric acid (saturated)
    - 25 ml Formaldehyde
    - 5 ml Acetic acid (glacial)

6 METHODS

6.1 Ethical statement

The care and treatment of animals was carried out in strict accordance with the Act No. 246/1992 Coll., on the protection of animals against cruelty. Official permission was issued to the Faculty of Science, Charles University in Prague by the Ministry of Education, Youth and Sports of the Czech Republic.

6.2 XtiSCs cultivation and preparation for microinjection and surgery

Sorted cells (XtiSCs-RFP) were cultivated in *Xenopus* testicular cell 2/3 cultivation medium in thermostat 29.5 °C and 5,5% atmospheric CO_2. Cultivation medium was changed 2 times a week. Cell culture was passaged weekly.

Medium was removed with Pasteur pipette and replaced with 5 ml of papain solution. After 10 min of papain activity, cell suspension was resuspended and transferred into 15ml tube with 5 ml of cultivation medium, which stopped enzymatic reaction. Subsequently, tube was centrifuged for 5 min at 900 revolutions per minute (rpm) (110x g), and supernatant fluid was discarded. Afterwards cells were resuspended in 1 ml of cultivation medium, and 200 µl of suspension was transferred back into cultivation flask. Remaining cells were used for further experiments (surgery) or CHIR99021 treatment and afterwards for experiments (microinjection, surgery). For surgery injection (not CHIR99021 treatment), cells had to be centrifuged for 5 min at 900 rpm (110x g), supernatant solution discarded, and cells resuspended in 2/3 PBS.

6.3 CHIR99021 treatment

To induce dedifferentiation (epithelial-mesenchymal transition), we passaged 20×10^6 cells into cultivation bottle and after 8-16 hours, XtiSCs were treated with 3µM CHIR99021 solution. Treatment procedure lasted for 72 hours. At the day of microinjection or surgery, cells were passaged, centrifuged for 5 min at 900 rpm (110 x g), supernatant solution discarded, and cells resuspended in 2/3 PBS.

6.4 IVF

One day before IVF, supervisor injected (priming injection) 30 units of human chorionic gonadotropin (hCG) subcutaneously into the dorsal lymph sac of female to prepare animal for ovulation. Followed by boosting injection of 300 units of hCG in the morning of the IVF procedure. When female kept at 25 °C, it began ovulating after 4-6 hours after the boosting injection.

For sperm source, male has to be euthanized and testes extracted. Male was placed into 0,4% MS222 bath (killing solution). After 10-15 min animal lost its leg reflexes when being grabbed by a leg, cervical spine section with immediate spinal cord disruption was performed with scissors and spike. Afterwards one pair of testes was extracted and stored in a 500 µl L-15 + 10% FBS medium.

When female started to lay eggs into water, it was ready for IVF. We prepared Petri dish (90mm) and put 3-5 ml of 1x MMR + Gentamycin solution into middle, this solution ensured delay in development and further synchronization of all oocytes. Female was grabbed into hand and faced posterior side down. After gentle squeezing, female started to lay eggs into Petri dish. Next, testes were homogenized, mixed with pipette and spread into a Petri dish between eggs. During that, eggs were placed into monolayer with pipette tip. When sperm was applied, it took 5 min to bound on eggs in the monolayer. For fertilization step, 0,05x MMR was added till Petri dish was full. After 20 min, solution was changed for 2,2% L-cysteine solution and together with embryos transferred into 250ml baker. For 5 min in baker, solution was gently mixed in a hand. This solution removed jelly coat from developing embryos and ensured cleanliness of the culture. To remove L-cysteine, embryos were washed 4 times with 0,05x MMR and transferred into agarose coated Petri dish with 0,05x MMR + gentamycin. This solution prevents developing embryos from any bacterial infections. Agarose coated Petri dish is used to prevent embryo´s damage, because when jelly coat is removed, embryos become fragile and adherent to plastic surface. Next, quality selection was made focusing on right cleavage of 4-8 cell stage embryos, colour and size. On the third day of cultivation, 0,05x MMR + gentamycin solution was replaced for 0,05x MMR without gentamycin to allow embryos gain their own microbiome.

6.5 Cell microinjection into tadpoles

Microinjection of XtiSCs-CHIR treated cells was performed by nitrogen-pressure controlled microinjector. Firstly, glass capillary was installed into injection holder and adjusted with tweezers into sharp tip for smooth injection. Afterwards small amount of cell suspension was sucked into injection capillary and output volume was set up by changing the pulse duration using the glass graticule. The pressure was constant approximately 8,8 psi. 40 nl of cell suspension (20×10^6 cells/ml) containing 1000 cells was injected into each tadpole. All microinjection experiments were done on tadpoles (stage 50+), which represents animals 2-3 weeks after IVF.

Tadpoles were placed into Petri dish coated with agarose and filled with saline water. Then 10-20 drops of 0.2% MS222, as an anaesthetic solution, were added. When tadpoles were immobilized, they were catched with holding capillary and placed with ventral side up (Fig. 5). Afterwards holding capillary with tadpole was placed on agarose surface and injection of XtiSCs into the heart ventricle was performed. Directly after injection we observed heart stopping for 8-15 sec, after which beating was recovered and capillary was pulled out from ventricle. Capillary pulled out after heart recovery, secured cells leaking from ventricle directly after injection. Tadpoles were then transferred into saline water with addition of Gentamicin (5 µl/ml) (V.M.D. n.v./s.a.). After 5-10 min, animals started to move in water without any visible limitation. Animals were subjected into XtiSCs, XtiSCs-CHIR, PBS injected and no microinjected groups.

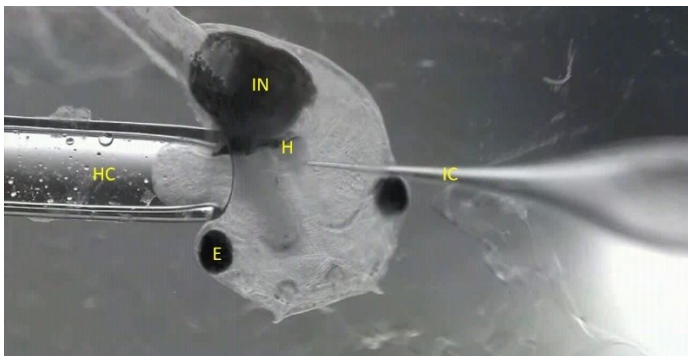

Figure 5. Transplantation (microinjection) of XtiSCs in the heart:
Tadpole is positioned ventral side up and anesthetized. IC- injection capillary, HC- holding capillary, E- eye, H- heart, IN- intestine.

6.6 Surgery, heart resection and transplantation experiments of adult *X. tropicalis*

Cell injection into the heart or skeletal muscle bed contained 10^6 cells in 50 µl of 2/3 PBS.

Female *X. tropicalis* was treated with MS222 (800 mg/L) bath. After 10-20 min (depends on size of animal), when animal lost its leg reflexes while being grabbed by a leg, it was transferred on surgical table. Animal was positioned ventral side up and limbs secured from movement. The skin in chest area was sterilized with iodine disinfection. A skin incision (V shape) was made over the heart using chirurgical scissors. Careful surgical cut was next performed on muscles without any damage of the mid-ventral vein. The pericardial sac was carefully open, and the heart ventricle was exposed. 2/3 PBS or cells were sucked into insulin syringe and injection of 50 µl 2/3 PBS or other groups was performed (Fig. 6. B). Afterwards, apex of heart ventricle was caught into tweezers and during the ventricle diastole, an amputation with chirurgical scissors was performed (Fig. 6. C). Approximately 5% of ventricle tissue from apex was dissected, followed with massive bleeding (Fig. 6. D). Within 30-60 sec, bleeding was stopped by rapid blood coagulation and pressed sterile cotton in wound area. The opened cavity and the skin were closed with three stiches of 2-0 multifilament silk suture (Fig. 6. F). The animal was immediately transferred into tank with saline water and Gentamycin (5 µl/mL) (V.M.D. n.v./s.a.). After 15-20 min, animal recovered from anaesthesia. All animals were monitored and fasted 24 hours after surgery.

First approach was injection directly into the heart before resection, as described. Second protocol of surgery was different in injection site, as injection was performed in skeletal muscle bed of hindlimb and afterwards resection protocol followed, as described previously. Third approach was injection into skeletal muscle bed, but three days before the apical resection. All procedures included ventricle resection. Animals were subjected into groups: XtiSCs-CHIR injected into heart, XtiSCs-CHIR injected into skeletal muscle, XtiSCs injected into heart, XtiSCs injected into muscle bed, XtiSCs injected into muscle 3 days before surgery, followed by PBS injections and no injury controls.

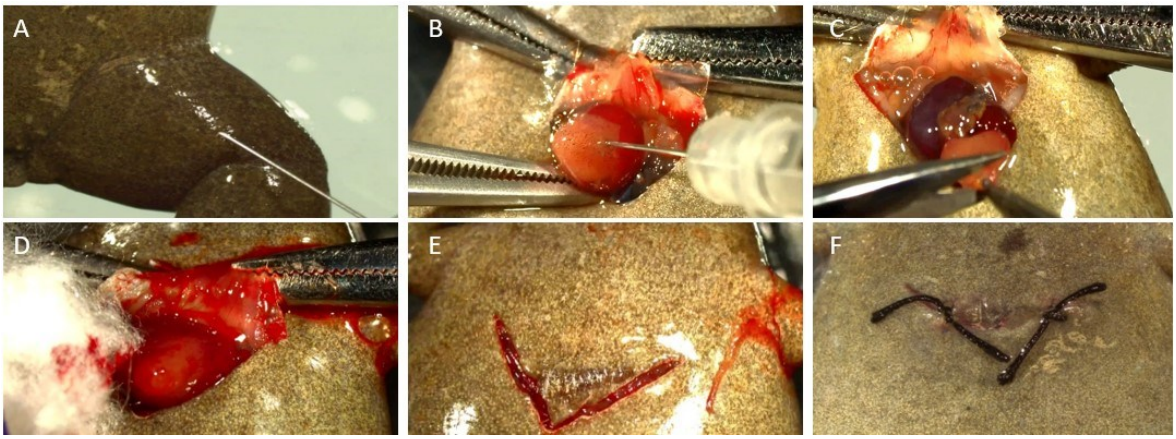

Figure 6. Apical resection of the adult *X. tropicalis* heart with XtiSCs transplantation: **(A)** Injection (transplantation) of the XtiSCs directly into skeletal muscle bed, **(B)** Injection (transplantation) of the XtiSCs directly into heart, **(C)** Apical resection of the heart, **(D)** The heart immediately after apical resection and bleeding stop with sterile cotton, **(E)** Muscle and skin incision after surgery, **(F)** Skin incision closed with stitches.

6.7 Tadpoles observation after microinjection

Tadpoles after microinjection procedure were observed under fluorescence stereomicroscope Olympus BX40 and were selected for positive RFP signal in the heart. During observation tadpoles were treated with few drops of sleeping solution MS222.

6.8 Adult frog heart observation after surgery

Adult frog was anesthetized with 0.4% MS222 (killing solution). After 10-15 min animal lost its leg reflexes when being grabbed by a leg, cervical spine section with immediate spinal cord disruption was performed with scissors and spike. Hearts were collected, washed in 2/3 PBS, cleaned from blood clot. Pericardium sac was removed and blood inside heart was carefully washed-away with 1 ml of 2/3 PBS injection into heart. Afterwards heart was observed under Stereomicroscope Stemi 2000.

6.9 Sample collecting and fixation

Tadpoles at given time points were fixed in 1x MEMFA + 3.7% Formaldehyde solution for 20 hours in 4 °C. Afterwards, samples were washed 3×5 min in 2/3 PBS and dehydrated in ascending concentrations of methanol for 5 min each (50%, 80%, 90%, and 100%)

at room temperature. For long term storage, samples in 100% methanol were placed in freezer (-18 °C).

Hearts from adult frogs were fixed for microtome and vibratome sectioning in 1x MEMFA + 3.7% Formaldehyde solution for 24 hours in 4 °C. Afterwards, samples were washed 3×5 min in 2/3 PBS and dehydrated in ascending concentrations of methanol for 5 min each (50%, 80%, 90%, and 100%) at room temperature. For long term storage, samples in 100% methanol were placed in freezer (-18 °C).

For cryotome sectioning hearts were fixed in 4% paraformaldehyde for 20 hours in 4 °C. Afterwards, washed 3×5min in 2/3 PBS and further processed in cryotome sample preparation, without any storage step.

6.10 Vibratome sectioning

All procedures were performed in room temperature if not mentioned otherwise.

6.10.1 Embedding sample into low melting agarose

Tadpoles/hearts stored in freezer (-18 °C) in 100% methanol were washed in descending concentrations of methanol for 5 min each (90%, 80% 50%) with final wash in 2/3 PBS for 5 min. The rehydrated sample was transferred into 15ml tube containing 10 ml of 4% low melting agarose in 1x PBS solution. The tube was placed in hybridization oven heated to 48.5 °C into rotary holder and set to lowest rpm. Sample was left in oven overnight for agarose saturation. Afterwards, sample was transferred to a 24-well culture plate and embedded in agarose in desired position. The plate was placed in freezer -18 °C for 10 min. Agarose block was then adjusted with razor and mounted to vibratome sectioning disc.

6.10.2 Sample sectioning

Before every sectioning it was necessary to calibrate vibratome. It was performed with razor mounted on vibratome´s cutting arm. In sectioning position, removable device VibroCheck measured vibrations in all directions of blade and all values were set to 0. Afterwards, sample mounted on sectioning disc was placed into vibratome tray, filled-up with cooled 1x PBS (4 °C). Tray was cooled by ice placed around. Then, operator set sectioning position

of calibrated razor, speed of sectioning arm (0.18-0.35 mm/s), amplitude (0.3-0.5 mm), and thickness of section (30-50 µm). Sections with thickens of 30- 50 µm were transferred from tray with glass pipette into cell strainer placed in 6-well plate.

6.10.3 Immunofluorescence of vibratome sections

Sections from vibratome were placed in 0.1% Triton X-100 solution diluted 1x with PBS for 1 hour. Followed by washing in 1x PBS 3×5 min. Blocking of non-specific binding sites which antibodies could bind, was performed in TNB solution for 1 hour. Afterwards, TNB solution was discarded and sections were incubated with primary antibodies (diluted to working concentration with TNB) 3 days at 4 °C. Then sections were washed in 1x PBS 3×5 min. Incubation with secondary antibodies (diluted to working concentration with TNB) was performed overnight at 4 °C. During secondary antibodies incubation, sections had to be covered with foil paper to avoid exposure to light and bleaching of fluorophores. Then sections were washed in 1X PBS 3×5 min, transferred to Super Frost Plus microscope slide, and mounted with mounting medium Mowiol with fluorescent dye DAPI. To finish immunofluorescence procedure sections were covered with cover glass and sealed with nail polish.

6.11 Microtome sectioning

All procedures were performed at room temperature if not mentioned otherwise.

6.11.1 Embedding sample into paraffin

Hearts stored in freezer (-18 °C) in 100% methanol were washed in descending concentrations of methanol for 5 min each (90%, 80% 50%) with final wash in 2/3 PBS for 5 min. Hearts were transferred in 75ml baker and dehydrated in ethanol ascending gradient for 10 min each (30%, 50%, 80%, 96%) and absolute ethanol 3×10 minutes. Afterwards, samples were transferred in benzene and washed 2×5 minutes. Then hearts were transferred in benzene-paraffin (1:1) in thermostat (58 °C) for 20 minutes. Samples were then put into preheated baker filled with clean paraffin for 1 hour (58 °C). During this process ceramic plate, which was covered with surface layer of paraffin oil,

was prepared. Ceramic plate was placed in thermostat to warm up to 58 °C, to prevent paraffin solidification on plate surface. After 1 hour, plate was filled up with clean paraffin and hearts were transferred on plate. Samples in paraffin-filed plate were stored for 15 hours in thermostat, to saturate sample with paraffin and excessed benzene evaporated. Afterwards, another ceramic plate surface was cover with paraffin oil and placed in thermostat to warm up to 58 °C. Then, plate was filled-up with fresh paraffin and samples were transferred on plate and oriented into desired position. Plate with samples was taken out from thermostat and set aside until paraffin started to stiffen from edges. When paraffin on surface solidified, plate was transferred into ice bath for fast cool down. Afterwards, samples were separated into paraffin blocks and mounted to wooden block (for microtome block clamp).

6.11.2 Sample sectioning

Before sectioning, samples attached to wooden blocks were transferred for 1 hour into freezer (-18 °C), to secure the most solid structure of paraffin. Samples were sectioned at microtome HM310 with thickness ≈6 μm and afterwards on microtome RM2255 with thickness ≈2 μm. Obtained sections were then transferred into cold water bath (15 °C) to secure good position on microscope slide. Then, sections from cold bath were transferred on microscope slide to warm water bath (45 °C), to allow sections to flatten. After few seconds, sections were transferred to clean microscope slide. For histological staining, were used microscope slide (P-Lab) and for antigen retrieval and immunofluorescence staining Super Frost Plus slides (Thermo Fisher Scientific). Afterwards, excess water was removed, and slides placed on heating plate (39 °C), to dry out sections.

6.11.3 Microscope slide coating for microtome sections

We used two approaches to secure a good adherence of sections to microscope slide. One approach was coating the slides with Gutenby´s glue or Gelatine glue. We dipped clean microscope slides into glue and let them dry out in thermostat (37 °C).

Another approach was focused on baking samples on slides. When sections dried completely on microscope slides, they were placed inside hybridization oven HO-10 for 8 hours (55 °C).

6.11.4 Histology staining

For Hematoxylin and Eosin staining, slides with sections were deparaffinized in xylene 3×10 min. Transferred to absolute alcohol 2×5 min and rehydrated in descending gradient of ethanol (96%, 80%, 50%) each 3 min and rinsed with tap water for 5 min. Next, slides were transferred in Gill´s hematoxylin for 30-40 min, depends on staining. Afterwards, hematoxylin was washed out with running tap water for 10 min. Differentiation of sections was performed in 1% HCl+80% ethanol solution for 3 sec. Then, slides were transferred in tap water and washed in running water for 1 min. Eosin staining was performed for 10 min followed with 5 min wash in running tap water. Afterwards slides were dehydrated in 96% ethanol for 5 min and 2×5 min in absolute ethanol. Followed with 3×5 min in xylene and mounted into mounting medium Entellan and cover with cover glass.

For Masson´s trichrome blue staining, slides with sections were deparaffinized in xylene 3×10 min. Transferred to absolute alcohol 2×5 min and rehydrated in descending gradient of ethanol (96%, 80%, 50%) each 3 min and rinsed with distilled water for 5 min. Next, sections were re-fixed in Bouin´s solution for 1 hour at 56 °C in hybridization oven HO-10. This step improves staining quality. Rinsed in running tap water for 5 min. Stained in Weigert´s hematoxylin for 10 min and rinsed in running tap water for 10 min. Next, slides were washed in distilled water and stained in Ponceau-Fuchsin for 10 min. Then, washed in distilled water and differentiate in 5% phosphomolybdic acid for 10-15 min or until collagen was not red. Slides were directly transferred into Aniline blue for 5-10 min. Next, rinsed in distilled water and differentiated in 1% acetic acid for 2-5 min and then washed in distilled water for 5 min. Afterwards slides were dehydrated in 96% ethanol for 20 sec and 2×5 min in absolute ethanol. Followed with 3×10 min in xylene and mounted into mounting medium Entellan and cover with cover glass.

6.11.5 Antigen retrieval

Formaldehyde fixation and paraffin embedding, cause epitope (antigen) cross-linking. This makes impossible for antibody to bond to its specific epitope. Thus, antigen retrieval techniques (physical, chemical and enzymatic) are employed to relax antigen cross-linking and uncover epitopes.

Slides with sections were deparaffinized in xylene 3×10 min. Transferred to absolute alcohol 2×5 min and rehydrated in descending gradient of ethanol (96%, 80%, 50%) each for 3 min and rinsed with distilled water for 5 min. Then, 600ml baker was filled up with 400 ml of distilled water and brought to a boil on induction cooker. Afterwards, slides were placed in rack and transferred into 150ml baker filled with antigen retrieval solutions (sodium citrate buffer, TE buffer or PBS buffer). Baker with slides was transferred into boiling water bath and antigen retrieval solution heated up to 95 °C. Temperature of antigen retrieval solution was regulated to not reach 100 °C, because boiling water would destroy sections on slides. Slides were incubated in 95 °C for 20 min. Next, baker with slides was transferred on ice and cooled down on room temperature.

6.11.6 Immunofluorescence of microtome sections

After antigen retrieval, sections were bounded with pap pen, which prevents leaking and reduce consumption of antibody solution. Next, sections were incubated in 0.1% Triton X-100 solution diluted 1x with PBS for 3×5 min. Then, blocked for non-specific binding sites, with 2% BSA for 1 hour. Afterwards, sections were incubated with primary antibody solution (diluted to working concentration with 2% BSA and 1x PBS) for 1 hour in wet chamber. Next, sections were incubated in 0.1% Triton X-100 solution diluted 1x with PBS for 3×5 min and incubated with secondary antibody solution (diluted to working concentration with 2% BSA and 1x PBS) for 45 min in wet chamber placed in dark to avoid exposure to light and bleaching of fluorophores. Then, sections were washed 3×5 min in 1x PBS. Then sections were incubated with anti-fading solution (5mM Cu_2SO_4 in 50mM ammonia acetate) for 30 min in wet chamber placed in dark. Mounting medium Mowiol with DAPI was applied and sections were covered with cover glass and sealed with nail polish.

6.12 Cryotome sectioning

All procedures were performed in room temperature if not mentioned otherwise.

6.12.1 Sample preparation for cryotome sectioning

Hearts were washed from paraformaldehyde fixation 3×5min in 2/3 PBS and transferred into ascending gradients of saccharose (5%, 10%, and 15%) for 2 hours each. Then, transferred into final 20% saccharose and left overnight in fridge (4 °C). Sagittal section of heart was performed, divided into 2 halves and mounted into O.C.T.™ Compound 4583 medium. Samples were then placed into freezer (-80 °C). Frozen sample was mounted on cryotome sectioning disk by O.C.T.™ Compound 4583 medium.

6.12.2 Sample sectioning

Cryotome temperature was set to -22 °C. Sample placed on cryotome sectioning disc was mounted into holder and sectioned in thickness of 8 µm. Every single section was transferred to warm Super Frost Plus slide, when it was enclosed to frozen section. Slides were transferred to freezer (-80 °C) and stored.

6.12.3 Immunofluorescence of cryotome sections

Cryotome sections were rinsed 3×5min in 1x PBS. To maintain the best structure of heart, sections were fixed on slide with 4% formaldehyde diluted with 1x PBS for 5 min. Afterwards washed 3×5min in 1x PBS and permeabilized in 1% SDS solution diluted with 1x PBS for 5 min. This step also works as antigen retrieval for formaldehyde fixed cryotome sections. Next, sections were washed 3×5min in 1x PBS. Then, blocked for non-specific binding sites, with 2% BSA for 1 hour. Afterwards, sections were incubated with primary antibody solutions (diluted to working concentration with 2% BSA and 1x PBS) for 1 hour in wet chamber. Next, sections were incubated in 0.1% Triton X-100 solution diluted 1x with PBS for 3×5 min and incubated with secondary antibody solutions (diluted to working concentration with 2% BSA and 1x PBS) for 45 min in wet chamber placed in dark to avoid exposure to light

and bleaching of fluorophores. Then, sections were washed 3×5 min in 1x PBS. Mounting medium Mowiol with DAPI was applied and sections were cover with cover glass and sealed with nail polish.

6.13 Area measurements and statistical analysis of heart sections

The measurement areas of fibronectin and cardiac tropomyosin were analysed on immunofluorescence longitudinal cryotome heart sections using NIH ImageJ software. Area on unedited picture was marked with free hand selection function regarding borders of fibronectin deposition on each section and this area was cleared from outside tissue and image has been saved as TIFF. Using colour threshold function, we selected only red areas of fibronectin and only green areas of cardiac tropomyosin. These areas were measured as a total area of injury and then separately for fibronectin and cardiac tropomyosin. Due to, non-automated measurement of areas, we got deviation ± 5% when calculated total area and fibronectin and cardiac tropomyosin together. Measurement was performed on three independent heart sections for XtiSC and PBS groups and one for non-operated control heart (CTRL). Total area ratios were then transferred to percentage. T-test was performed to compare XtiSC and PBS groups regarding the fibronectin and cardiac tropomyosin areas.

7 RESULTS

7.1 Localization and proliferation of XtiSCs-RFP treated with CHIR99021 in the heart of tadpole (stage 50+)

To elucidate if CHIR treatment do not negatively influence survival of XtiSCs in *in vivo* conditions, we transplanted XtiSCs-CHIR inside heart. Further, we wanted to clarify if cells are capable of proliferation inside tadpole. All these data obtained from tadpole experiments were used in adult *X. tropicalis* experiments. Transplantation experiments were performed with immature Sertoli cells derived from *X. tropicalis* testicles. XtiSCs were microinjected into hearts of tadpoles (stage 50+). This stage has been selected since it is transparent, and heart is developed enough to withstand microinjection (injury) with glass capillary. 40 nl of 2/3 PBS with 1000 cells was injected directly into heart. After injection and cell delivery we observed heart stop, which has been recovered within 10 sec. Afterwards, colonization and proliferation of cells was observed. Proliferation of cells was observed from 1st day after microinjection until 30th day after microinjection (Fig. 7), since all tadpoles were sacrificed at 30th day after microinjection. Cells were mainly localized in the area of heart. However, some cells were found outside heart muscle, such as around heart and eyes.

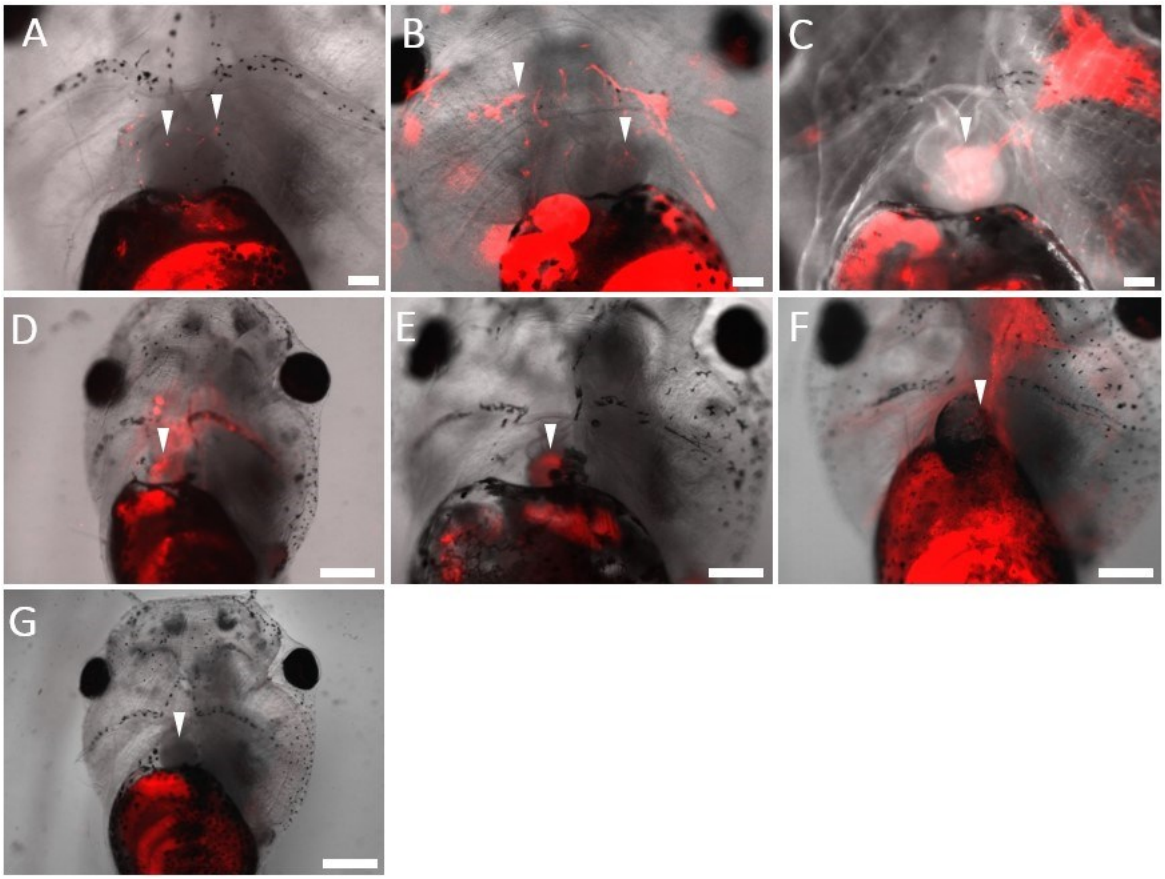

Figure 7. Proliferation of XtiSCs-RFP after transplantation into the heart of *X. tropicalis* tadpole (stage 50+): (A) 2 hours after XtiSCs transplantation, cells are localized in the heart or heart area (white arrows), (B) 1 day after XtiSCs transplantation, cells start to proliferate, (C) 4 days after XtiSCs transplantation, (D) 7 days after XtiSCs transplantation, (E) 10 days after XtiSCs transplantation, (F) 30 days after XtiSCs transplantation, (G) Tadpole injected with 2/3 PBS into the heart (white arrow), red autofluorescence under heart is caused by bacteria inside intestine. Scale bar: 200 µm.

7.2 Heart colonization of tadpole (stage 50+) by XtiSCs-RFP treated with CHIR99021

Fluorescent stereomicroscope figures can demonstrate proliferation of XtiSCs, but localization of cells with this technique is not appropriate, because it cannot be exactly defined if cells are localized above heart or inside heart. Thus, we used technique of vibratome sectioning and immunofluorescence staining to determine heart colonization with XtiSCs (Fig. 8). At 1st day after transplantation cells were localized inside heart muscle (Fig. 9. A4). At 7th day after transplantation, cells survived inside heart and proliferated

(Fig. 9. B4). At 30th day after transplantation cells colonized heart, but also outgrowth area around heart (Fig. 9. C4).

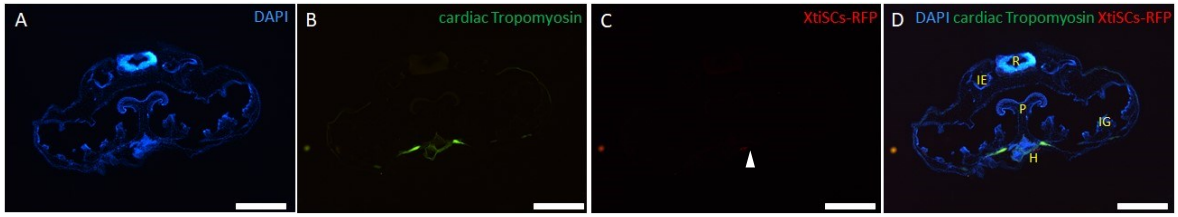

Figure 8. Immunofluorescence analysis of tadpole´s vibratome cross section at 1 day after transplantation:
(A) positive immunofluorescence of DAPI, **(B)** positive immunofluorescence of cardiac Tropomyosin, **(C)** positive immunofluorescence of RFP, **(D)** merge of A, B, C. (H- heart, P- pharynx, IG- internal gills, IE- inner ear, R- rhombencephalon), (Blue- nuclei, Green- cardiac muscle, Red- XtiSCs) Scale bar: 250 µm.

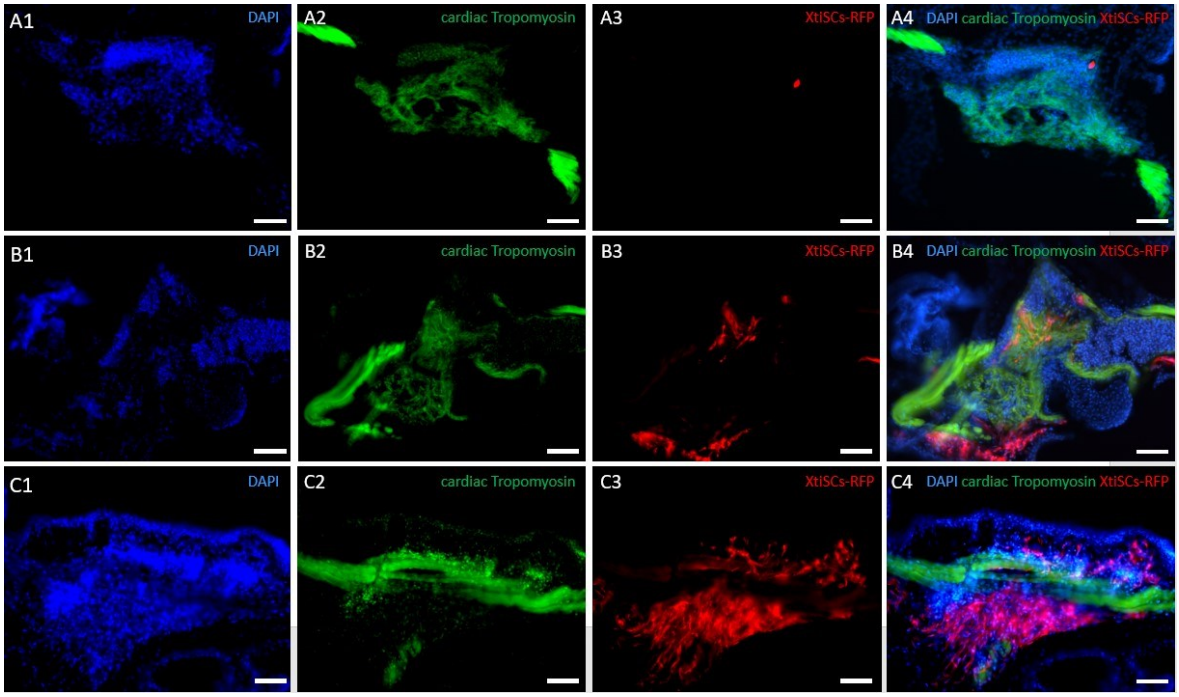

Figure 9. Immunofluorescence analysis of tadpole´s vibratome cross sections:
(A1-A4) 1 day after transplantation, **(B1-B4)** 7 days after transplantation, **(C1-C4)** 30 days after transplantation. (Blue- nuclei, Green- cardiac muscles, Red- XtiSCs) Scale bar: 50 µm.

7.3 Apical resection of adult *X. tropicalis* heart

Apical resection of adult *X. tropicalis* heart, is complicated surgery. First of all, it was complicated to specify appropriate concentration of MS222, which anaesthetized and did not kill adult female. Final concentration was set at 800 mg/L. Another obstacle was to use vital individuals. Firstly, Nosek (8 years old) strain was used. Unfortunately, survival rate was low after apical resection and most of dead animals were represented by this strain (Fig.10). Afterwards, Nigerian strain was used. These animals were 4 years old and vital. However, we observed differences in reactions to anaesthesia in smaller and more robust individuals. Effect of anaesthesia, in case of smaller individuals was rapid fall asleep and weak heartbeat. Most of small individuals did not recover from anaesthesia.

All adult animals used in thesis underwent removal of approximately 5% of ventricular tissue from heart apex. The resection damaged ventricle and was followed by massive bleeding. Bleeding was stopped by applying pressure with sterile cotton in wound area for 30-60 sec. After blood clot formation, heart beating remained normal in robust individuals, whereas in smaller individual the heartbeat weakened. The standardized protocol of apical resection surgery resulted in 62% survival rate (37 individuals survived from 60 operated) (Fig.10). However, survival rate of the three last surgeries was over 90 % (data not published).

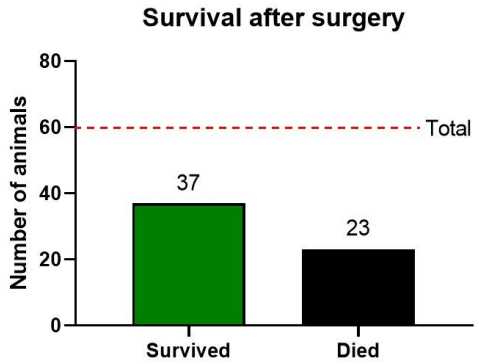

Figure 10. Graphical representation of survival after heart surgery:
Total number of animals used for apical resection of ventricle was 60, from which 37 individuals survived and 23 died. Created in GraphPad 8.0.1.

7.4 Transplantation of XtiSCs in adult *X. tropicalis*

Transplantation experiments were performed with immature Sertoli cells derived from *X. tropicalis* testicles. Firstly, one million XtiSCs treated with CHIR and in other group without treatment (in 50 µl of 2/3 PBS) were injected directly inside heart/bloodstream. We have expected direct differentiation of XtiSCs-CHIR into cardiomyocytes. However, we did not observe any survived cells in the heart or wound area (data not published). Due to this result, we have changed injection site to skeletal muscle bed. We did not expect differentiation but rather production of growth factors and signalling molecules supporting the potential cardiomyocyte proliferation and healing by XtiSCs-CHIR, such as MSCs treatment of heart failure (Shabbir *et al.*, 2009). This approach was successful in cells survival in muscle bed 7 days after transplantation (Fig.11.A3). Also results of fibrotic scar formation 7 days after apical resection and transplantation of XtiSCs-CHIR into skeletal muscle bed, demonstrated lower fibrotic scar formation, but results differed to much in this experimental approach (Fig.12.C1). Next, we focused on secretome of paracrine factors and immunomodulatory effect of Sertoli cells. We injected XtiSCs without CHIR treatment into skeletal muscle bed. However, this group was not used, due to non-survived individual. On the other hand, inflammatory response after apical resection or heart failure is rapid and if cells are transplanted at time of injury, results in reaction time could differ. Therefore, we injected XtiSCs three days before apical resection. Transplanted cells survived in skeletal muscle bed for 10 days (Fig. 11. B3) Thus, XtiSCs were not recognized by immune system and destroyed. Results of morphological fibrotic scar formation in this group were consistent (Fig. 12. D1) and displayed the lowest scar deposition from all groups.

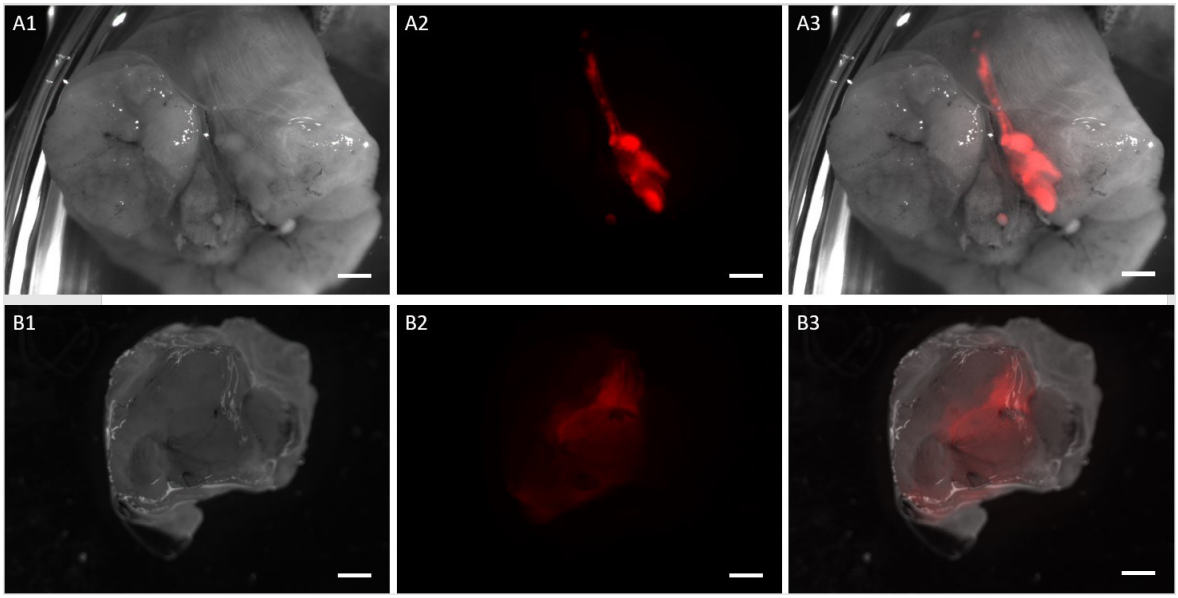

Figure 11. Localization and survival of XtiSCs in skeletal muscle bed:
(A1-A3) Survival of XtiSCs treated with CHIR99021 7 days after injection, **(B1-B3)** Survival of XtiSCs without CHIR99021 treatment 10 days after injection. Scale bar: 1 mm.

7.5 Fibrotic scar formation 7 days after apical resection

The morphology of hearts was examined at 7 days after apical resection. Heart injected with XtiSCs-CHIR (Fig. 12. A1-A2) XtiSCs (no CHIR treatment) (Fig. 12. B1-B2) display wide scar formation, such as heart injected with 2/3 PBS (Fig. 12. E1-E2). If XtiSCs-CHIR were injected in skeletal muscle bed during heart surgery (Fig. 12. C1-C2), hearts of adults display lower scar formation within 7 days after injury. On the other hand, if XtiSCs (no CHIR) were injected in skeletal muscle bed 3 days before surgery, fibrotic scar formation seemed to be inhibited to minimum (Fig. 12. D1-D2).

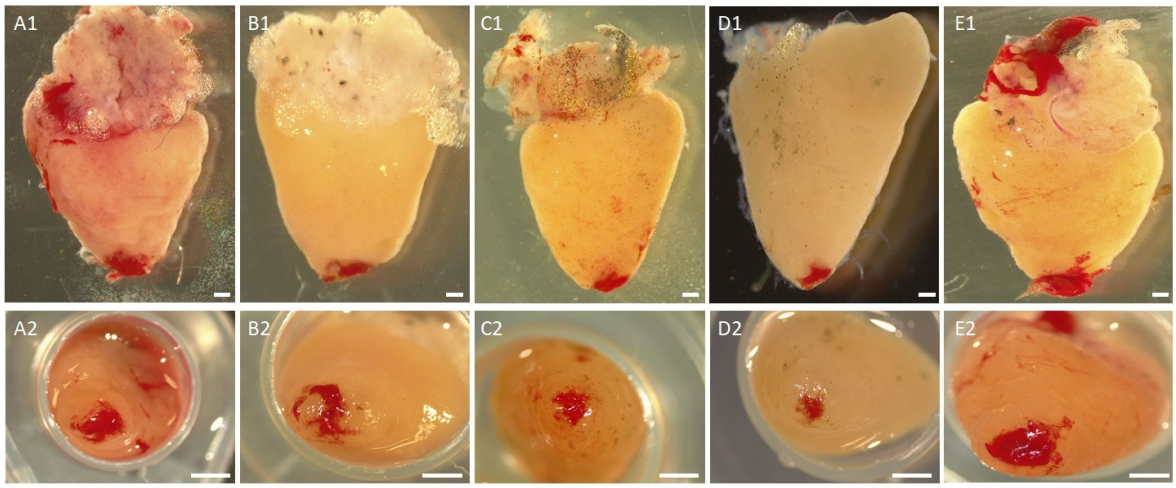

Figure 12. Fibrotic scar formation at 7 days after apical resection:
(A1) Injured heart, which was injected with XtiSCs-CHIR into heart, **(A2)** Detail view of heart apex of A1, **(B1)** Injured heart, which was injected with XtiSCs (no CHIR treatment) into the heart **(B2)** Detail view of heart apex of B1, **(C1)** Injured heart, XtiSCs-CHIR were injected into skeletal muscle bed during surgery, **(C2)** Detail view of heart apex of C1, **(D1)** Injured heart, XtiSCs (no CHIR treatment) were injected into skeletal muscle bed 3 days before surgery, **(D2)** Detail view of heart apex of D1, **(E1)** Injured heart which was injected with 2/3 PBS, **(E2)** Detail view heart apex of E2. Scale bar: 1 mm.

7.6 Standardization of sectioning technique of adult heart sample

For tadpole sections, we used vibratome, which gave us appropriate quality of cross section structure, good affinity of antibodies and no autofluorescence. For adult heart sectioning, were used three different techniques: 1. Vibratome, 2. Microtome, and 3. Cryotome.

7.6.1 Vibratome

For heart embedding, 4% low melting agarose was used. Low melting agarose secured good manipulation with sample even at lower temperatures. This also helped to set the correct position of sample to obtain best sections. Even though, sample was in right position and properly embedded, vibrations of blade during sectioning destroyed heart structure. The structure was so destroyed that it could not be used for further analysis, even if we tried different settings of vibratome´s blade amplitude or speed. Next, sections from vibratome were too thick (30-60 µm) and incubation with antibodies was complicated because we used incubation in strainers and not on microscope slides. On the other hand, some sections were mounted on slide and analysed. These sections had appropriate specific binding

of antibodies with good fluorescence (Fig. 13). Almost no autofluorescence was observed. However, as mentioned previously, structure of longitudinal section was damaged.

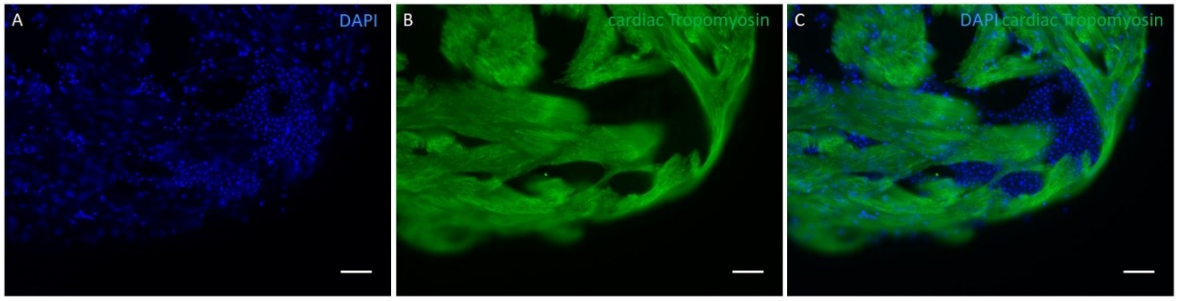

Figure 13. Immunofluorescence analysis of longitudinal undamaged vibratome section of the heart:
(A) positive immunofluorescence of DAPI, **(B)** positive immunofluorescence of cardiac Tropomyosin, **(C)** merge of A, B. DAPI outside of heart represent nuclei of red blood cells. Scale bar: 50 µm.

7.6.2 Microtome

Paraffin embedded samples for microtome sectioning underwent 24 hours fixation with 4% formaldehyde, but also incubation with benzene and high temperatures in thermo box (56-59 °C) during sample saturation with paraffin. These procedures secured excellent thin sections (2-6 µm) with perfect morphological structure. Microtome sections were used for Hematoxylin & Eosin (Fig. 14) and Masson´s trichrome (blue) (Fig. 15) histological staining. Hematoxylin & Eosin staining is classical histological staining, but it uses only two colours resolution (nuclei- blue, cytoplasm-pink) and it was not enough for fibronectin and collagen resolution. Thus, protocol for histological staining was changed to more complex Masson´s trichrome (blue) staining. Masson´s trichrome uses three histological colours: Hematoxylin, Ponceau-Fuchsin, and Aniline blue. This technique offers also staining of fibronectin and collagen (Nuclei-brown, Cytoplasm-dark pink, Fibronectin/Collagen- blue).

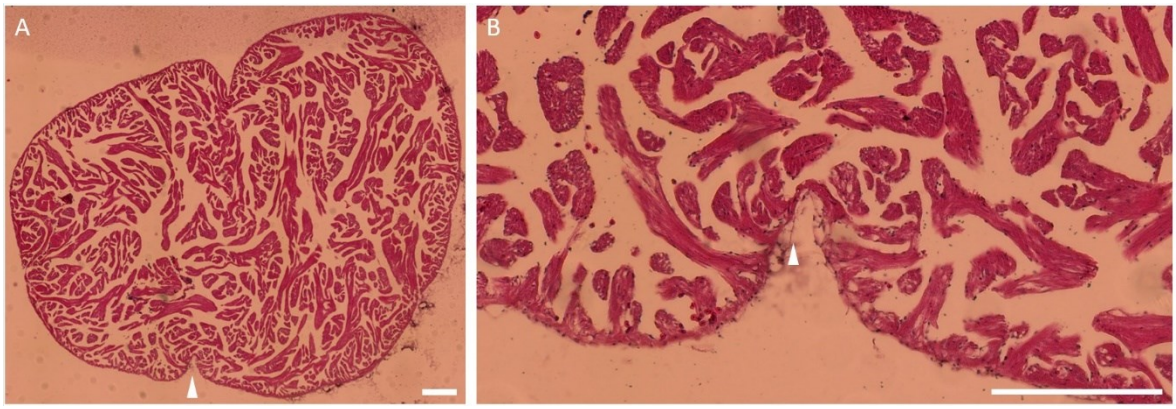

Figure 14. Hematoxylin & Eosin staining of adult *X. tropicalis* heart, 1 day after apical resection:
(A) Longitudinal section of an adult heart at 1 day after apical resection. Incision was performed only on limited area, arrow points to wound area, **(B)** Detail of injury area, arrow point to small depositions of fibronectin (white), cardiac tissue (pink), nuclei (blue). Scale bar: 400 µm.

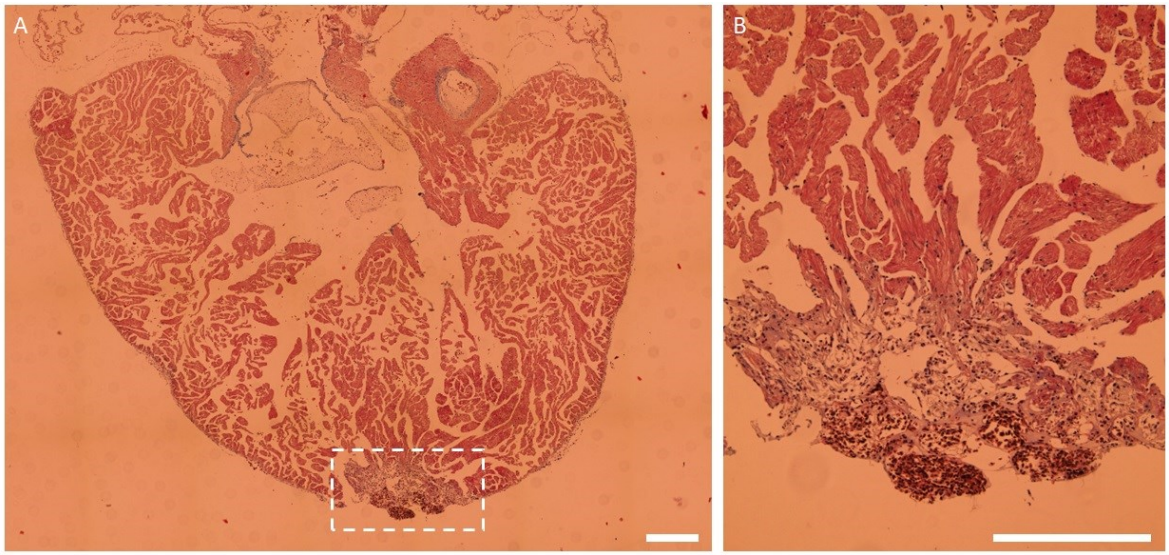

Figure 15. Masson´s trichrome (blue) staining of adult *X. tropicalis* heart, 7 days after apical resection:
(A) Longitudinal section of an adult heart at 7 day after apical resection. Highlighted area demonstrates resection site, **(B)** Distinguishing of fibronectin/collagen deposition (light blue) from cardiac tissue (pink) is more appropriate than in case of Hematoxylin & Eosin staining. Nuclei (brown). Scale bar: 400 µm.

Next, we analysed microtome sections with immunofluorescence. However, specific binding of primary antibodies to epitopes is blocked, due to formaldehyde fixation and techniques associated with paraffin embedding. These procedures cause epitope cross-linking and mask antigenic sites. Antigen retrieval methods break these

cross-linking and expose antigenic sites. Thus, antibody can bind to its specific epitope afterwards.

The two main methods for antigen retrieval are heat induced retrieval and enzymatic retrieval. To obtain the best morphology of section we used heat induced antigen retrieval, since enzymes also partially destroy section structure. We have tested 3 different solutions, such as Sodium citrate buffer (pH=6), TE buffer (pH=9), and PBS buffer (pH=7.5). Due to, heating process we have also tested different coated slides with Gutenby´s glue, gelatine glue and Super Frost Plus slides (Thermo Fisher Scientific), which should prevent sections falling from slide during heating process. Sections during retrieval in TE buffer always washed away without dependence on slide coating. In case of Sodium citrate buffer and PBS buffer the best results were obtained with Super Frost Plus slides (Thermo Fisher Scientific). Nevertheless, immunofluorescence of sections was not optimal (Fig. 16). High intensity of sample autofluorescence made any analysis unable. For this reason, we have tested, incubation with anti-fading solution for 30 min after secondary antibody application. Anti-fading solution suppressed autofluorescence of section. However, specific immunofluorescence signal was also reduced but distinguishable (Fig. 17). When all these obstacles were overcome, we found inconsistent staining of sections. It could be caused by improper antigen retrieval, or damaged epitopes by heating. Immunofluorescence results of microtome sections were not used for analysis, due to complicated preparation and inconsistent staining.

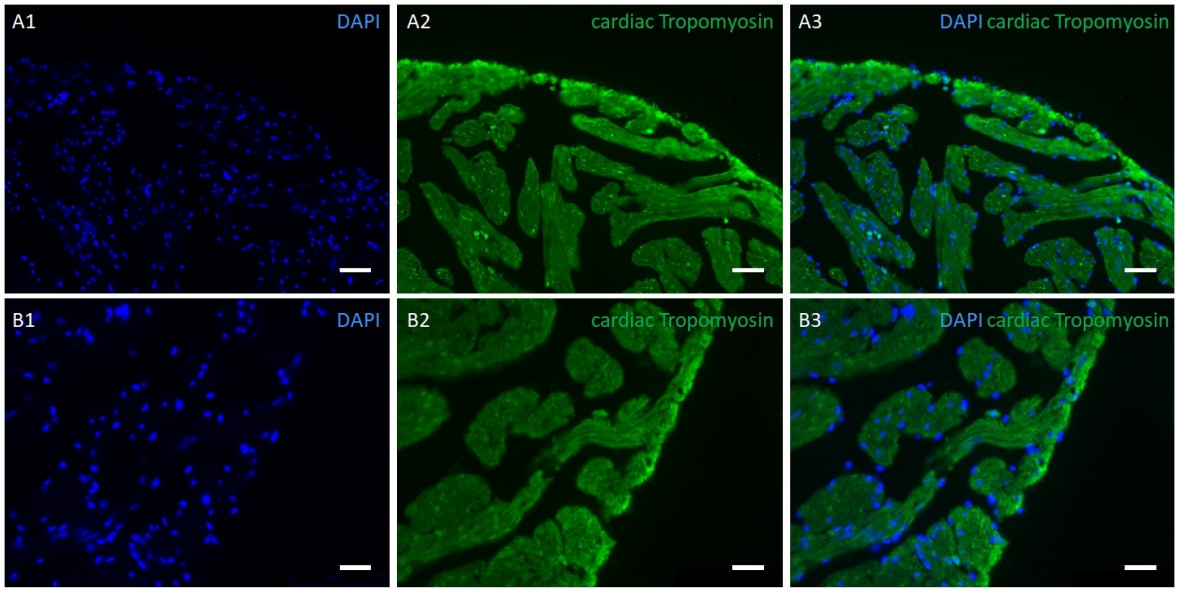

Figure 16. Immunofluorescence of microtome sections of heart (no injury) after antigen retrieval and without antifading solution:
(A1) positive immunofluorescence of DAPI, **(A2)** positive immunofluorescence of cardiac Tropomyosin, **(A3)** merge of A1, A2 and antigen retrieval with PBS buffer, inconsistent fluorescence in border zone and inside of section **(B1)** positive immunofluorescence of DAPI, **(B2)** positive immunofluorescence of cardiac Tropomyosin, **(B3)** merge of B1, B2 and antigen retrieval with Sodium Citrate buffer, inconsistent fluorescence in border zone and inside of section. Scale bar: 50 µm.

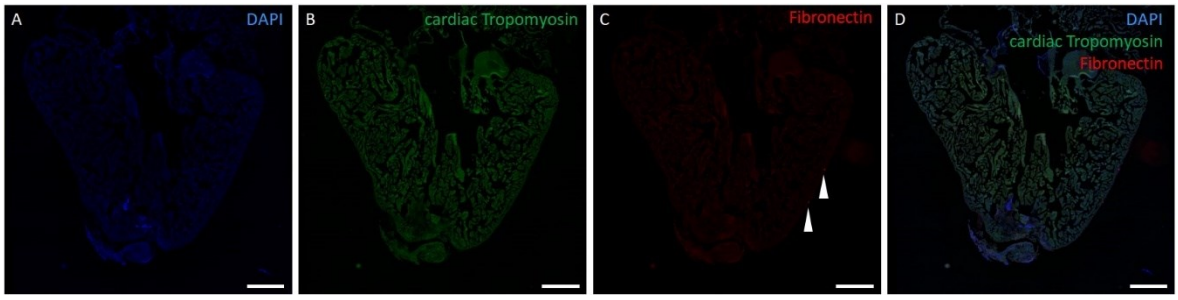

Figure 17. Immunofluorescence of microtome section heart (PBS injected in the heart) after antigen retrieval and antifading solution:
(A) positive immunofluorescence of DAPI, **(B)** positive immunofluorescence of cardiac Tropomyosin, **(C)** positive immunofluorescence of Fibronectin (white arrows points to only specific bindings of antibody) **(D)** merge of A, B, C and antigen retrieval with Sodium Citrate buffer, inconsistent fluorescence. Scale bar: 400 µm.

7.6.3 Cryotome

Fixation solution for cryotome samples were changed from 1x MEMFA + 3.7% formaldehyde to 4% paraformaldehyde. Paraformaldehyde fixation secures lower

epitope cross-linking but still preserves good quality of morphology. Further, process of sample embedding for cryotome is much gentle, than in case of microtome. Due to these gentle processes, cryotome sections are suitable for immunofluorescence analysis.

Fixed samples were saturated in successive concentrations of saccharose (5%, 10%, 15%, and 20%). Saccharose secured sample freeze without formation of crystals, which would otherwise damage sample structure. Afterwards, samples were transferred directly into O.C.T.™Compound medium and placed in freezer (-80 °C). Embedded samples were then sectioned on cryotome (8 µm thick) and further analysed.

Paraformaldehyde fixation is much gentle to epitopes, but still causes cross-linking. Due to this, sections had to undergo antigen retrieval, but not by heating. Antigen retrieval for cryotome sections consists of incubation in 1% SDS solution for 5 min in room temperature. This process bypasses problems with reproducibility due to consistent conditions compared to antigen retrieval by heating. Immunofluorescence of sections was uniform and without autofluorescence (Fig. 18).

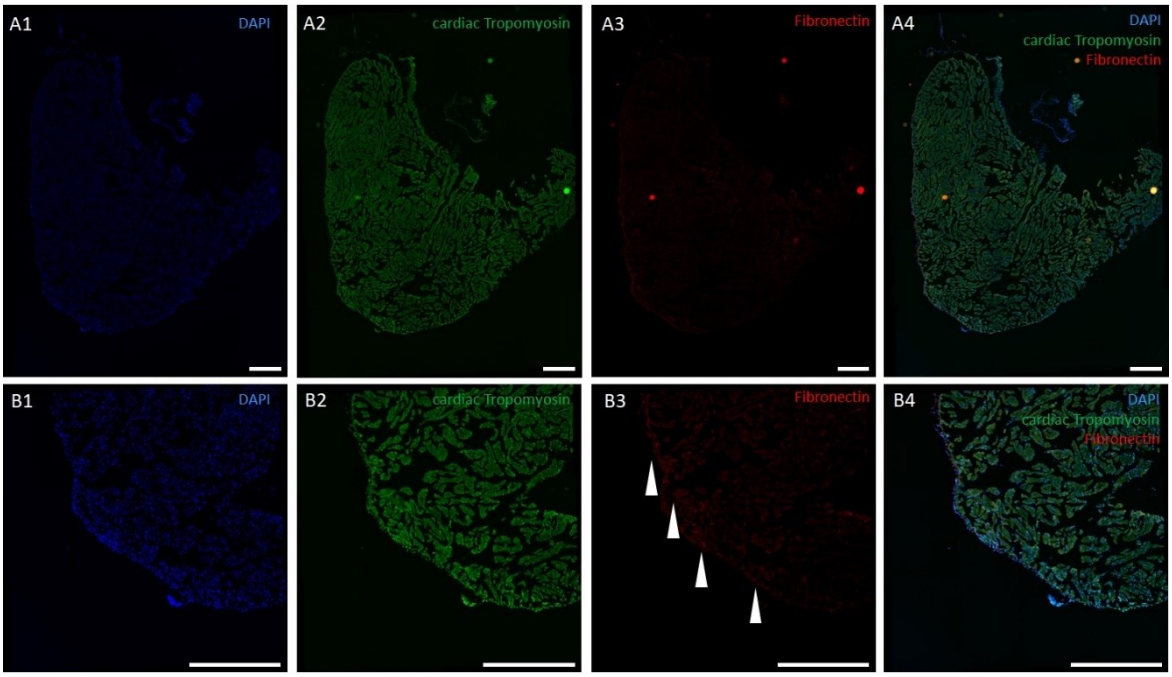

Figure 18. Immunofluorescence of cryotome control non-operated heart (CTRL) heart section: (A1) positive immunofluorescence of DAPI, whole heart section, **(A2)** positive immunofluorescence of cardiac Tropomyosin, whole heart section, **(A3)** positive immunofluorescence of fibronectin, whole heart section, **(A4)** merge of A1, A2, and A3, whole heart section, **(B1)** positive immunofluorescence of DAPI, detail of heart apex, **(B2)** positive immunofluorescence of cardiac Tropomyosin, detail of heart apex, **(B3)** positive immunofluorescence of fibronectin, detail of heart apex, **(B4)** merge of B1, B2, and B3, detail of heart apex. (Blue- nuclei, Green- cardiac muscles, Red- XtiSCs) Scale bar: 400 µm.

7.7 Characterization of ECM (fibronectin/collagen) deposition 7 days after apical resection of adult *X. tropicalis* heart

After standardization of sectioning and staining techniques, we analysed fibronectin deposition in the heart apex 7 days after apical resection. Firstly, XtiSCs treatment of heart injury was focused on direct injection of cells inside heart and differentiation into cardiomyocytes. Due to, low differentiation potential of XtiSCs, cells were treated with GSK-3 inhibitor, CHIR99021. This drug triggers epithelial-mesenchymal transition (EMT), which shifts XtiSCs into mesenchymal-like phenotype and promotes differentiation potential of XtiSCs (Nguyen *et al.*, 2019). However, analysis revealed no XtiSCs localization in wound area or inside heart of adult *X. tropicalis* (not published data).

Histological Masson´s trichrome (blue) staining revealed that, hearts injected directly with XtiSCs-CHIR (Fig. 19. C1), displayed similar damaged structure as hearts injected with PBS (Fig. 19. B1). On the other hand, if injection of XtiSCs after CHIR treatment was performed inside skeletal muscle bed during surgery, hearts exhibited much better morphological structure healing 7 days after apical resection, but still with high ECM deposition levels (Fig. 19. D1).

Due to these results, we assumed that, XtiSCs transplantation (with/without CHIR treatment) with direct injection into the heart and differentiation into cardiomyocytes is not effective. If hearts injected directly with PBS and XtiSCs displayed similar damaged morphology, we supposed high death rate of cells during transplantation, similarly to MSCs transplantation experiments done by Freyman *et al.* (2006) and Toma *et al.* (2009).

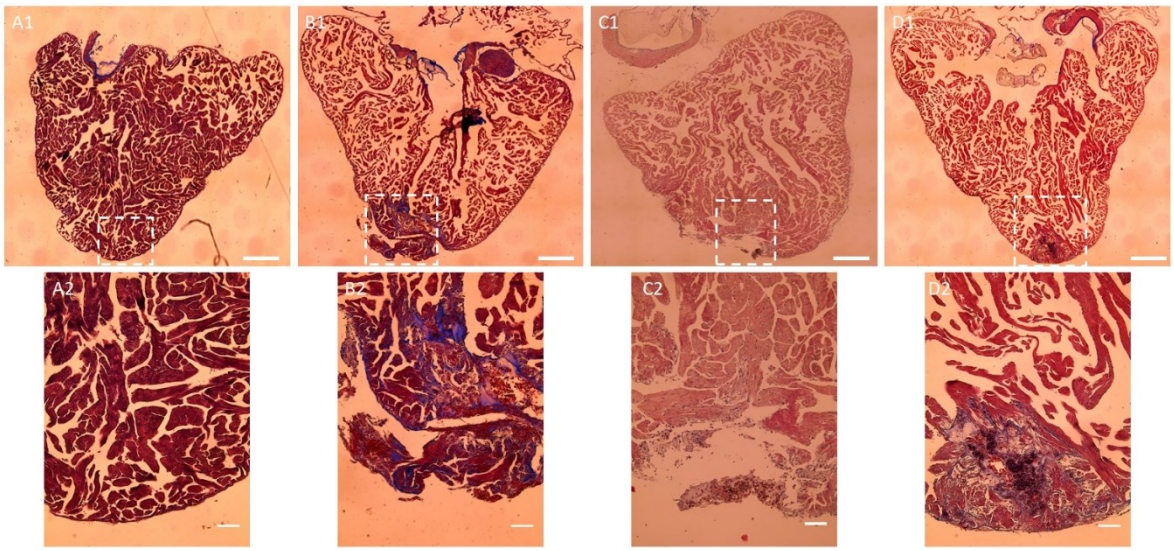

Figure 19. Fibronectin/collagen deposition 7 days after apical resection of adult *X. tropicalis* heart and injection of PBS/XtiSCs (Masson´s trichrome blue):
(A1) CTRL heart, **(A2)** detail of CTRL heart apex, **(B1)** Operated heart, PBS injection into heart, **(B2)** detail of B1 heart apex, **(C1)** Operated heart, XtiSCs after CHIR treatment injected into heart, **(C2)** detail of C1 heart apex, **(D1)** Operated heart, XtiSCs after CHIR treatment injected into skeletal muscle bed during surgery, **(D2)** detail of D1 heart apex. Brown- nuclei, pink/dark pink- cytoplasm, blue- fibronectin/collagen. Scale bar A1, D1: 400 µm. Scale bar A2, D2: 50 µm.

Results indicated promising experimental approach of XtiSCs transplantation into skeletal muscle bed, with their possible paracrine effect of Sertoli cells, which can boost cardiac regeneration. Thus, we targeted therapy into remote control by secreted paracrine factors of XtiSCs. Moreover, we excluded CHIR treatment, since it promoted differentiation potential, but it also reduced the production of paracrine factors secreted by XtiSCs. We injected XtiSCs 3 days before apical resection into skeletal muscle bed, to let them recover from transplantation. At the day of the surgery we performed only apical resection.

Individuals, which underwent XtiSCs pre-treatment 3 days before surgery into muscle bed (Fig. 20. C4/D4) displayed lower fibronectin deposition levels, compared to individuals treated with PBS injection (Fig. 20. A4/B4) 7 days after apical resection.

Further, area measurements of cryotome sections at site of apical resection (Fig. 20) confirmed significantly lower levels of fibronectin deposition ($P<0.05$) and higher levels of cardiac muscles (cardiac Tropomyosin) ($P<0.05$) after XtiSCs injection into skeletal muscle bed compared to PBS injection 7 days after surgery (Fig. 21).

Direct injection of XtiSCs displayed no successful colonization of wound area in the heart. Heart injection with PBS or XtiSCs displayed similar damaged structure at injury site 7 days after apical resection. Due to, these data, Sertoli cell immature phenotype

and immunomodulatory capacity of these cells we retreated from CHIR99021 treatment, which transforms cells into MSC-like phenotype, which was mainly focused to direct differentiation to cardiomyocytes. On the other hand, injected adult animals with XtiSCs into skeletal muscle bed 3 days before surgery significantly decreased fibronectin deposition 7 days after surgery ($P<0.05$), which is main prerequisite for successful heart regeneration. All these data partially confirmed hypothesis, that transplanted XtiSCs are capable to positively influence cardiac regeneration after injury, if cells were injected inside skeletal muscle bed of adult *X. tropicalis*.

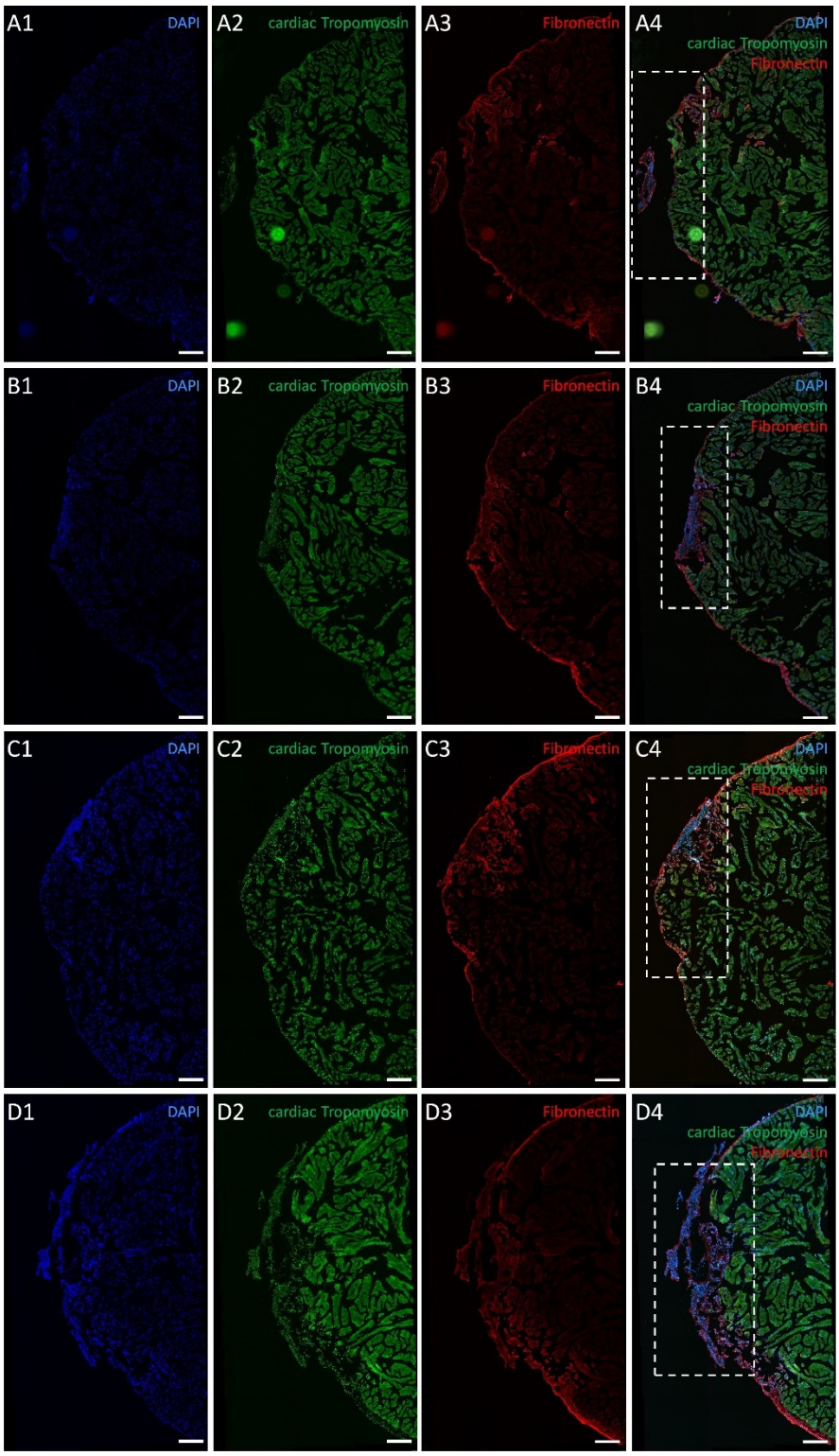

Figure 20. Fibronectin deposition 7 days after apical resection of adult *X. tropicalis* heart (10 days after PBS/XtiSCs injection into skeletal muscle bed):
(A1-A4 and B1-B4) immunofluorescence of longitudinal heart sections from two adult frogs 7 days after apical resection and 10 days after PBS injection into skeletal muscle bed. **(C1-C4 and D1-D4)** immunofluorescence of heart sections from two adult frogs 7 days after apical resection and 10 days after XtiSC injection into skeletal muscle bed. **(A1-D1)** DAPI staining, **(A2-D2)** immunofluorescent staining of cardiac Tropomyosin, **(A3-D3)** immunofluorescent staining of Fibronectin, **(A4-D4)** merge. Scale bar: 200 µm.

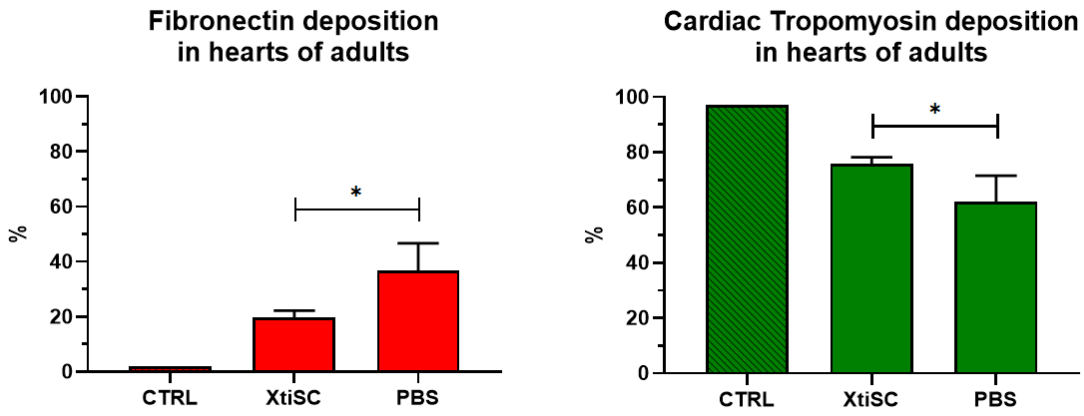

Figure 21. Comparison of cardiac tropomyosin and fibronectin deposition in the hearts of adults:
Non-operated heart (CTRL), Adult hearts 7 days after apical resection with XtiSCs transplantation into skeletal muscle bed 3 days before surgery (XtiSC), Adult hearts 7 days after apical resection with PBS injection into skeletal muscle bed 3 days before surgery (PBS). Fibronectin represents ECM deposition level, cardiac tropomyosin represents cardiac muscle deposition level. Created in GraphPad 8.0.1.

8 DISSCUSSION

To investigate the heart regenerative potential of *Xenopus tropicalis* immature Sertoli cells (XtiSCs), we have established two injury models. The first was embryonic model, which was represented by tadpole (stage 50+) and the second was an adult frog (4 years old). Tadpoles were microinjected with 1000 cells directly inside the heart and myocardium was damaged by the incision with injection capillary. On the other hand, adult frogs were injected with 10^6 cells directly inside the heart or skeletal muscle bed and the cardiac ventricle was damaged by apical resection of ventricle.

In testicles, Sertoli cells protects newly formed germ cells, by formation of BTB and immunomodulatory function of immune system (O'Bryan *et al.*, 2005; reviewed in Kaur *et al.*, 2014). Immunoprotective ability of Sertoli cells is not limited only to testes. Transplantation of bovine adrenal chromaffin cells into rat's brain resulted in total rejection of xenotransplanted cells, but if chromaffin cells were co-transplanted with Sertoli cells, both cell types survived in the brain over 2 months. Moreover, Sertoli cells significantly reduced immune response, if compared to only chromaffin cells transplantation alone (Sanberg *et al.*, 1996). Furthermore, survival of allogenic heart grafts into mouse was prolonged after Sertoli cells injection (Lim *et al.*, 2009). Immunomodulatory capacity of Sertoli cells was further demonstrated by Lee *et al.* (2008), as Sertoli cells inhibited activation and maturation of dendritic cells in presence of lipopolysaccharides. Regulation of immune system was performed by suppression of up-regulation of CD40 on dendritic cells. Moreover, Fallarino *et al.* (2009), performed transplantation of immature Sertoli cells into mouse with type 1 diabetes. Cells injected into peritoneal cavity reversed diabetes with no need of additional insulin therapy. Furthermore, β-cells function of insulin secretion, was completely recovered. All these data demonstrate, that Sertoli cells create immune-privileged environment within testes, by mechanical barrier and modulation of immune system response. However, what is more surprising is that, these cells are capable to retain these properties outside the testicles.

Sertoli cells were thought to be terminally differentiated cells with nourishing function for germ cells (Dufour *et al.*, 2003). In our laboratory, XtiSCs were characterized as precursors of Sertoli cells and for further analysis, RFP gene was inserted under CAG promotor into genome of XtiSCs. These cells express pluripotency marker *klf4*, *tert*, and *c-myc*. However, expression of other pluripotency markers, such as *oct4* and *sox2*,

were reduced. Further, analysis confirmed immature Sertoli cells phenotype and somatic origin (Tlapakova *et al.*, 2016). To improve differentiation potential, XtiSCs were treated with GSK-3 inhibitor CHIR99021, which promotes EMT and shifts XtiSCs into MSC-like phenotype. After this treatment XtiSCs are capable to differentiate into chondrocyte, osteocytes, adipocytes *in vitro* and cardiomyocytes *in vivo* after microinjection into tadpole (Nguyen, 2019). Thus, after CHIR treatment of XtiSCs, we targeted therapy to direct differentiation into cardiomyocytes after heart injury.

Adult mammals lost the capacity to fully regenerate cardiac muscle after myocardial injury. Instead of complete regeneration, they compensate lost cardiac tissue with fibrotic scar tissue which results in impaired heart contractility and mechanical function or eventually death. (reviewed in Porrello & Olson, 2014). However, Porrello and colleagues (2011, 2013) demonstrated that, neonatal mouse is capable to fully regenerate lost cardiac tissue 7 days after birth. ECM deposition after cardiac injury secures wall stiffness and protects ventricle from rupture, but persistent fibrosis causes regeneration failure (Marshall *et al.*, 2017). Moreover, excessive fibrosis after cardiac injury causes limited heart function and natural regeneration failure in medaka. On the other hand, zebrafish, which is closely related to medaka has capacity to completely regenerate damaged heart. However, if process of immune cell infiltration is delayed in zebrafish, it similarly to medaka results in excessive scarring and regeneration failure (Poss *et al.*, 2002; Lai *et al.*, 2017). For successful regeneration, ECM deposition has to be removed and replaced by new cardiomyocytes (Poss *et al.*, 2002; Lai *et al.*, 2017; Garcia-Puig *et al.*, 2019).

According to latest research, *X. tropicalis* adults can partially regenerate heart within 30 days after apical resection with low levels of persistent scar fibrosis (Liao *et al.*, 2017). In addition, experiments by Lv and colleagues (2020) demonstrated that, cardiac telocytes are localized in the heart of adult *X. tropicalis* and might play a role in cardiac regeneration. However, ECM deposition is still present, and the heart function after apical resection was not analysed in these publications (Liao *et al.*, 2017; Lv *et al.*, 2020). Thus, reduction of excessive fibronectin is first step to improve heart regeneration in adult *X. tropicalis*. It was demonstrated, that modulation of immune response in medaka, reduced fibrosis and improved cardiac regeneration (Lai *et al.*, 2017). Also, XtiSCs have immunomodulatory capacity and we assumed, that after transplantation into adult *X. tropicalis*, they can influence fibronectin deposition. Moreover, we tested differentiation

potential of XtiSCs in adult´s heart and then compared fibronectin levels between frogs after apical resection, which received XtiSCs or PBS injection.

For *in vivo* differentiation experiments of XtiSCs treated with CHIR in adult *X. tropicalis* heart, we had to test survival of cells after this treatment in tadpole´s heart. They are more accessible, transparent and their immune system is not developed enough, which on the other hand secures also capacity of limb regeneration (Fukazawa *et al.*, 2009). XtiSCs differentiation experiments in tadpoles were performed by Nguyen (2019), who confirmed that, XtiSCs after CHIR treatment are able to differentiate into cardiomyocytes after microinjection into peritoneum at stage 41. Prolonged survival and proliferation of cells, together with experiments done by Nguyen (2019) confirmed, that XtiSCs-CHIR are able to proliferate *in vivo* within 30 days after microinjection into the heart (Fig. 7). Further immunofluorescence analysis proved that, proliferating cells are incorporated inside heart (Fig. 9) and can differentiate into cardiomyocytes in embryo (Nguyen, 2019).

All these data allowed us to move to experiments on adult *X. tropicalis*. Here we faced to many obstacles. Firstly, protocols for surgery, apical resection of ventricle, and cells delivery into adult animal were not introduced in our laboratory and we followed surgery protocol done by Liao and colleagues (2017). They used anaesthetic concentration of 1000 mg/L (MS 222) and ice-cooled operation table for 12 months old female *X. tropicalis*. However, our animals which underwent anaesthesia and surgery were 8 years old and most of them did not survived. Thus, we used younger 4 years old animals to which we adjusted the MS222 at concentration 800 mg/L and did not use ice-cooled operation table. This concentration and surgery procedure displayed much better survival rate (Fig. 10). On the other hand, variations in size of individuals also contributed on survival rate. If frogs were bigger, their heartbeat was much stronger after the chest opening and these animals had much better chance to survive surgery, than smaller animals with weak heartbeat. This also correlated with results of male *X. tropicalis* surgery, since males were smaller and none of operated individual did not survived. Thus, all experiments were done on 4 years old females.

Other obstacles were cell delivery directly inside heart and apical resection of ventricle. Injection into the heart was difficult to perform, because heart was still beating, and we had a problem to aim the syringe needle and pierce it. On the other hand, cell delivery inside skeletal muscle bed was easy to perform, and it could be done without anaesthesia

if cells were applied 3 days before surgery. Apical resection of ventricle had to be carried out very carefully, because if we cut too much tissue, animals bleed out. On the other hand, if we cut just a small piece of tissue, results could be misleading. Thus, reproducibility of cell delivery and apical resection was one of the main goals.

Resection of the heart apex in zebrafish, causes massive bleeding, which is stopped by rapid blood coagulation. After 2-4 dpa, fibronectin incorporates into blood clot and cardiac muscle. Fibronectin deposition level reaches its maximum at 7 dpa and by 30 dpa almost all fibronectin is replaced by cardiac muscle. Completely regenerated apex occurs at 60 dpa (Poss *et al.*, 2002; Chablais & Jaźwińska, 2012). Further, *X. tropicalis* also displays maximal level of fibronectin deposition at 7-8 days after apical resection (Liao *et al.*, 2017). Due to this, we set our collection time of adult hearts at 7 days after apical resection, because we compared effect of transplanted XtiSCs on fibronectin deposition levels.

The first approach of heart injury treatment was focused on direct differentiation of XtiSCs into cardiomyocytes. For this purpose, cells were treated with CHIR and after 3 days treatment, delivered directly inside heart and as a control we injected also XtiSCs without CHIR treatment and PBS. However, no RFP positive cells were localized in the heart or in injury site (data not published). Moreover, fibrotic scar formation after XtiSC-CHIR or XtiSCs injection displayed similar morphology as in control animals (PBS injection) (Fig. 12. A1-A2, B1-B2, and E1-E2). We concluded that, most of cells did not survived transplantation into blood stream or were caught inside lungs similarly to intravenous MSCs delivery done by Freyman *et al*. (2006) and Toma *et al.* (2009).

It is important to note that intracoronary, intramyocardial or injection directly inside the heart are invasive methods of cell delivery with low levels of cell survival and can cause excessive damage, scar tissue, and arrythmia (Hagège *et al.*, 2006). Thus, the second approach of XtiSCs treatment was focused on a remote control and less invasive cell delivery into skeletal muscle bed during surgery. Experiments done by Shabbir and colleagues (2009) confirmed that, MSCs injected into skeletal muscle bed, after myocardial injury, increased levels of circulating trophic factors, such as HGF, leukemia inhibitory factor (LIF), and macrophage colony-stimulating factor (M-CSF). MSCs trophic factors further activated expression of HGF, insulin-like growth factor II (IGF-II), and vascular endothelial growth factor (VEGF) in the heart. In addition, 1 month after MSCs delivery, heart function was significantly improved with reduced fibrosis by 50% and 50% higher levels of cardiac

muscle (Shabbir *et al.*, 2009). Injection of XtiSCs-CHIR into skeletal muscle during surgery displayed better morphological structure of the regenerated heart and lower fibrotic scar formation 7 days after apical resection (Fig. 12. C1-C2) but results in this group has high variation and we were not able to characterize paracrine effect of XtiSCs-CHIR on scar formation. On the other hand, none of adult frogs injected with XtiSCs in skeletal muscle bed survived. However, all frogs in this group were small sized and during surgery they displayed weak heartbeat, so deaths in this group was not caused by the cell injection, but rather by weak individuals.

The last approach of cardiac injury treatment was injection of XtiSCs in skeletal muscle bed 3 days before apical resection. For this purpose, we decided to test only XtiSCs as an example of Sertoli cells therapy. We targeted therapy into remote control by secreted paracrine factors of XtiSCs and excluded CHIR treatment, since it promotes differentiation potential, but it also reduces the production of paracrine factors secreted by XtiSCs. Reason to choose time point of 3-day pre-treatment was to let cells properly incorporate into muscle bed and recover from injection. We did not choose longer time for pre-treatment, because from previous experiments we observed, that cells are able to survive 7 days in muscle (Fig. 11 A1-A3) and we were not sure, if they can survive for a longer time period. Analysis in this case confirmed that, XtiSCs survived in muscle bed for 10 days (Fig. 11. B1-B3). Fibrotic scar formation and morphological structure of the heart displayed preliminary results that, XtiSCs pre-treatment could reduce scar formation 7 days after apical resection (Fig. 12. D1-D2). Thus, we assumed that, pre-treatment and remote control of scar formation by XtiSCs could also influence the heart regeneration in adult *X. tropicalis*.

8.1 Optimization of adult heart sectioning and further analysis

For analysis of adult heart, we used three different methods of heart sectioning. The first method was Vibratome. Sections prepared with this technique are thick (30-50 μm) and can be damaged during free-floating incubation with antibodies or by vibrating razor during cutting. However, vibratome sections are suitable for immunofluorescence analysis, because the sample preparation does not cause high cross-linking of epitopes. Due to the relatively large section thickness, it needs to be incubated for a longer period of time with antibodies, which allows good penetration through the whole section (Ward *et al.*, 2008). For sample embedding low melting agarose is traditionally used

(Shim, 2011). This agarose secures low temperature for manipulation with sample during embedding. However, vibrating razor and incubation of free-floating sections destroyed structure of heart longitudinal sections.

Other procedures that could affect the sections quality are sample fixation and storage. In general, fixation by formaldehyde reduces immunoreactivity of epitopes but preserves structure. Moreover, prolonged fixation causes irreversible cross-linking of some epitopes (Arnold *et al.*, 1994; Webster *et al.*, 2009). It would be possible to reduce cross-linking by antigen retrieval techniques (enzymatic or heating) (reviewed in Shi *et al.*, 2001). However, sections structure was already damaged by razor and antibody incubations and further processing would destroy it completely. In addition, sample storage is also key step for successful vibratome sectioning. In this case samples were dehydrated after fixation and stored in 100% methanol. Absolute methanol is good at preserving antigenicity but can cause tissue shrinking. Thus, possible replacement would be with 50% or 70% methanol, which also preserves good antigenicity and structure of brain sections (Yuan *et al.*, 2017). Methanol is toxic and dangerous for a long-term work. Since ethanol is harmless it can serve as a full-fledged replacement in the same 70% concentration (Ward *et al.*, 2008).

The second method for heart sample sectioning was microtome. Microtome specimens are embedded in paraffin. Key steps for good quality sections, are sample dehydration and saturation by paraffin (Ward *et al.*, 2008). If sample was dehydrated incorrectly, it would result in wrong paraffin saturation and formation of cavities and subsequent sample crumbling. At correctly set temperatures and good paraffin saturation, it is possible to obtain section 2-5 μm thick with excellent morphology. Despite complex preparation, paraffin embedded specimens are still widely used in histology. If samples are stored in proper conditions, it is possible to use them 7 years for DNA sequencing and clinical diagnostics (Nagahashi *et al.*, 2017).

We wanted to use microtome sections for immunofluorescence analysis. Since formaldehyde fixation and chemical processing of paraffin embedding cause high levels of epitope cross-linking, it was necessary to use antigen retrieval by heating (reviewed in Shi *et al.*, 2001). Firstly, we struggled with section fixation on slide, as all sections washed away during antigen retrieval. Thus, we applied slide coating by gelatine glue and Gutenby´s glue. However, these coating methods did not work. Matsui *et al.* (2015) tested different commercially available slides coated with silane,

aminopropyltriethoxysilane, poly-L-lysine, and Thinlayer Advanced Cytology Assay System (TACAS) . TACAS displayed the best adhesion of sections but it was not available in Czech Republic at the time of the project. Other commercially available coated slides are Super Frost Plus slides (Thermo Fisher Scientific), which were used for paraffin sections of teeth and immunohistochemical analysis (Kjær & Nolting, 2009). Thus, we decided to use these slides, but they did not work either. Another widely used method, which prevents detaching , is baking sections on slides in oven (Syrjänen & Syrjänen, 1986). This method with combination of Super Frost Plus slides finally secured sections adhesion during antigen retrieval.

Immunofluorescence analysis of paraffin embedded sections revealed high autofluorescence in green and red channel. Yang *et al*. (2017) tested different techniques to reduce autofluorescence of paraffin embedded placenta sections by ultraviolet photobleaching, Sudan black B treatment, trypan blue treatment, copper (II) sulphate treatment and commercially available TrueBlack lipofuscin autofluorescence quencher solution (TLAQ). Sudan black B, copper (II) sulphate and TLAQ displayed the best results in autofluorescence reduction without reduction of specific fluorescent signal. Thus, we applied antifading copper (II) sulphate solution, which reduced autofluorescence to minimum, but also reduced specific fluorescent signal (Fig. 17). Processing of paraffin embedded samples was time consuming. Moreover, immunofluorescent results were not appropriate, and we struggled with distinguishing specific and unspecific signals. Afterwards we decided to use cryotome sections for immunofluorescent staining. However, paraffin embedded samples were suitable for histology, since they secure perfect preservation of structure.

Cryotome was the third method used for adult heart sectioning. The advantage is the relatively short time needed for the sample preparation. Sectioning, staining and observation can be carried out in one day. Procedures for sample embedding are much gentle compared to microtome, without any dehydration, so antigenicity is well preserved. (Fischer *et al.*, 2008). Marshall *et al*. (2017) used paraformaldehyde fixation and cryotome sectioning for immunofluorescence analysis of *X. laevis* hearts. We followed exact procedures step-by-step, from fixation, sample saturation by saccharose, mounting to OCT medium, sectioning, antigen retrieval and immunofluorescence staining. We verified that, this method is not time consuming, since we were able to finish

all procedures from sample collection to observation within 3 days. Furthermore, antigenicity preservation of section is superior and without any autofluorescence (Fig. 16).

8.2 Stem cell therapy and regeneration

MSCs are widely used in regenerative research and not restricted only to heart regeneration. Traumatic corneal injury could cause blindness. To test corneal therapy Du and colleagues (2009) injected human corneal stem cell directly inside corneal stroma of the lumican-null mice. Lumican is a major proteoglycan of corneal ECM. It organizes stroma and maintain corneal transparency by exact alignment of collagen fibres. Lumican-null mice developed corneal opacity, which mimics scar tissue. After stem cell delivery, mice restored thickens of corneal stroma and defects in collagen fibrils alignment. Moreover, transparency of cornea was equal to wild-type mice (Du *et al.*, 2009).

Further, MSCs or rather their extracellular vesicles were used in therapy of acute kidney injury. Extracellular vesicles enriched with exosomes by ultracentrifugation were injected intravenously in mice with acute kidney injury. Improvement of renal function was distinguishable within 2 days. Molecular analysis of extracellular vesicles enriched with exosomes revealed high concentration of messenger ribonucleic acids (mRNAs), which promoted cell cycle entry and progression, and regulate antiapoptotic and proliferative mechanisms (Bruno *et al.*, 2017).

Stem cells-based therapies are nowadays accompanied also in acute liver injury. Untreated injury can result in hepatocytes death, which can be partially reduced by drugs. However, more promising way to rescue hepatocytes is stem cell delivery inside organism. In murine acute liver injury model, MSCs were injected inside tail-vein. Cells were initially trapped in lungs but progressively migrated to wounded liver within 2 hours. MSCs further downregulated necrosis, inflammation, apoptosis and promoted hepatocyte renewal (Chetty *et al.*, 2019).

Pneumonia is nowadays the world-wide problem since pandemic of SARS-CoV-2 virus strikes to the all continents. Latest research demonstrated potential employment of MSCs within pneumonia. COVID-19 disease causes high inflammatory response and cytokine storm. As already described, MSCs display immunomodulatory capacity and secures healing in many other organs. Leng *et al.* (2020) intravenously injected 10^6 cells

per kilogram of patient´s weight. All patients were positive for COVID-19 and had symptoms, such as weakness, fever, and shortness of breath. Seven patients underwent MSCs therapy and three patients received placebo. Patients who received MSCs transplantation recovered from disease within 2-4 days after injection. Moreover, cytometry analysis of peripheral blood revealed high levels of overactivated T cells and natural killer cells before MSCs therapy and its drop out after therapy. Furthermore, regulatory T cells and dendritic cells levels increased after cell injection. Also, pro-inflammatory cytokine TNF-α was decreased after therapy and anti-inflammatory IL-10 together with growth factor VEGF markedly increased. Thus, MSCs therapy modulate overreaction of immune system and launches repair or regenerative processes. Moreover, MSCs can infiltrate lungs which can protects pulmonary microenvironment, prevent pulmonary fibrosis and improve respiratory function (Leng *et al.*, 2020).

Despite of a lost capacity to regenerate heart in adult mammals, Zhao and colleagues (2016) applied MSCs therapy to 8 weeks old mice after MI. MSCs exhibited secretory function of paracrine factors, which further increased cardiomyocyte survival rate. MSCs secretome disposed various cytokine and growth factors with cardio protective effect (Zhang *et al*., 2015b). It was demonstrated that, HGF is one of the key cardio protective cytokine from MI or ischemia (Arechederra *et al.*, 2013). And further experiments clarified, that MSCs are able to secrete HGF and attenuate apoptosis of cardiomyocytes by upregulation of AKT and downregulation of Bax and Bcl-2 (Shabbir *et al.*, 2009; Zhao *et al.*, 2016).

We accompanied these data, but we changed the source of cells to immature Sertoli cells. These cells or their conditioned medium were applied previously in regeneration of testicular microenvironment, where they restored germ cell production in azoospermic mouse (Panahi *et al.*, 2020). Moreover, transplantation of Sertoli cells into testicles of mouse, which underwent Sertoli cells depletion, resulted in repopulation of testicles and restoration of spermiogenesis (Yokonishi *et al.*, 2020). However, we were first group who applied Sertoli cells regarded to heart injury. We observed reduction in fibronectin deposition and increase in cardiac muscle levels within 7 days after heart injury, if cells were injected 3 days before injury inside skeletal muscle bed. This is first step in evaluation of immunomodulatory and regenerative capacity of XtiSCs regarded to heart. However, much deeper and detailed research is needed.

9 CONCLUSION

- Microinjection of XtiSCs-RFP into the heart of *X. tropicalis* tadpole (stage 50+) was standardized.
- Apical resection procedure of the heart was standardized for 4 years old *X. tropicalis* female.
- It was demonstrated that, XtiSCs after CHIR99021 treatment could survive and proliferate in the *X. tropicalis* tadpole´s (stage 50+) heart for 30 days after intracardial microinjection.
- Adult *X. tropicalis* heart sectioning was optimized. Paraffin embedded and microtome sectioned samples are suitable for histological analysis. Cryo-sections are suitable for immunofluorescence analysis. However, vibratome sections of adult heart displayed excessive damage. On the other hand, vibratome sections of tadpoles displayed excellent morphology.
- Injected XtiSCs (without CHIR99021 treatment) 3 days before apical resection displayed significant reduction of fibronectin deposition and increased cardiomyocyte proliferation in the wound area 7 days after apical resection if compared with uninjected or PBS injected experimental groups.

10 REFERENCES

Abdi, R., Fiorina, P., Adra, C.N., Atkinson, M. & Sayegh, M.H. (2008) Immunomodulation by mesenchymal stem cells: A potential therapeutic strategy for type 1 diabetes. *Diabetes*, **57**, 1759–1767.

Agata, K., Saito, Y. & Nakajima, E. (2007) Unifying principles of regeneration I: Epimorphosis versus morphallaxis. *Development Growth and Differentiation*, **49**, 73–78, (Review).

Arechederra, M., Carmona, R., González-Nuñez, M., Gutiérrez-Uzquiza, Á., Bragado, P., Cruz-gonzález, I., Cano, E., Guerrero, C., Sánchez, A., López-Novoa, J.M., Schneider, M.D., Maina, F., Muñoz-Chápuli, R. & Porras, A. (2013) Met signaling in cardiomyocytes is required for normal cardiac function in adult mice. *Biochiica et Biophysica Acta*, **1832**, 2204–2215.

Arnold, M.M., Srivastava, S., Fredenburgh, J., Stockard, C.R., Myers, R.B. & Grizzle, W.E. (1994) Effects of fixation and tissue processing on immunohistochemical demonstration of specific antigens. *Biotechnic and Histochemistry*, **71**, 224–230.

Arslan, F., Smeets, M.B., O'Neill, L.A.J., Keogh, B., McGuirk, P., Timmers, L., Tersteeg, C., Hoefer, I.E., Doevendans, P.A., Pasterkamp, G. & De Kleijn, D.P.V. (2010) Myocardial ischemia/reperfusion injury is mediated by leukocytic toll-like receptor-2 and reduced by systemic administration of a novel anti-toll-like receptor-2 antibody. *Circulation*, **121**, 80–90.

Bai, L., Lennon, D.P., Caplan, A.I., Dechant, A., Hecker, J., Krasno, J., Zaremba, A. & Miller, R.H. (2012) Hepatocyte growth factor mediates MSCs stimulated functional recovery in animal models of MS. *Nature Neuroscience*, **15**, 862–870.

Bajaj, P., Schweller, R.M., Khademhosseini, A., West, J.L. & Bashir, R. (2014) 3D biofabrication strategies for tissue engineering and regenerative medicine. *Annual Review of Biomedical Engineering*, **16**, 247–276, (Review).

Baratelli, F., Lin, Y., Zhu, L., Yang, S.-C., Heuzé-Vourc'h, N., Zeng, G., Reckamp, K., Dohadwala, M., Sharma, S. & Dubinett, S.M. (2005) Prostaglandin E 2 induces FOXP3 gene expression and T regulatory cell function in human CD4 + T cells. *The Journal of Immunology*, **175**, 1483–1490.

Becker, T., Wullimann, M.F., Becker, C.G., Bernhardt, R.R. & Schachner, M. (1997) Axonal regrowth after spinal cord transection in adult zebrafish. *The Journal of Comparative Neurology*, **377**, 577–595.

Bergmann, O., Bhardwaj, R.D., Bernard, S., Zdunek, S., Barnabé-Heider, F., Walsh, S., Zupicich, J., Alkass, K., Buchholz, B.A., Druid, H., Jovinge, S. & Frisén, J. (2009) Evidence for cardiomyocyte renewal in humans. *Science*, **324**, 98–102.

Bergmann, O., Zdunek, S., Felker, A., Salehpour, M., Alkass, K., Bernard, S., Sjostrom, S.L., Szewczykowska, M., Teresa, J., Remedios, C. dos, Malm, T., Andrä, M., Jashari, R., Nyengard, J.R., Possnert, G., Jovinge, S., Druid, H. & Frise, J. (2015) Dynamics of cell generation and turnover in the human heart. *Cell*, **161**, 1566–1575.

Bouffi, C., Bony, C., Courties, G., Jorgensen, C. & Noël, D. (2010) IL-6-dependent PGE2 secretion by mesenchymal stem cells inhibits local inflammation in experimental arthritis. *PLOS ONE*, **5**, https://doi.org/10.1371/journal.pone.0014247.

Bruno, S., Tapparo, M., Collino, F., Chiabotto, G., Deregibus, M.C., Lindoso, R.S., Neri, F., Kholia, S., Giunti, S., Wen, S., Quesenberry, P. & Camussi, G. (2017) Renal regenerative potential of different extracellular vesicles populations derived from bone marrow mesenchymal stromal cells. *Tissue Engineering: Part A*, **23**, 1262–1273.

Bryant, S. V., Endo, T. & Gardiner, D.M. (2002) Vertebrate limb regeneration and the origin of limb stem cells. *International Journal of Developmental Biology*, **46**, 887–896, (Review).

Bujak, M., Dobaczewski, M., Chatila, K., Mendoza, L.H., Li, N., Reddy, A. & Frangogiannis, N.G. (2008) Interleukin-1 receptor type I signaling critically regulates infarct healing and cardiac remodeling. *The American Journal of Pathology*, **173**, 57–67.

Cano-Martínez, A., Vargas-González, A., Guarner-Lans, V., Prado-Zayago, E., León-Olea, M. & Nieto-Lima, B. (2010) Functional and structural regeneration in the axolotl heart (*Ambystom mexicanum*) after partial ventricular amputation. *Archivos de Cardiología de México*, **80**, 79–86.

Chablais, F. & Jaźwińska, A. (2012) The regenerative capacity of the zebrafish heart is dependent on TGF- bet signaling. *Development and Stem Cells*, **139**, 1921–1930.

Chablais, F., Veit, J., Rainer, G. & Jaź, A. (2011) The zebrafish heart regenerates after cryoinjury- induced myocardial infarction. *BMC Developmental Biology*, **11**, https://doi.org/10.1186/1471-213X-11-21.

Chassot, B., Pury, D. & Jaźwińska, A. (2016) Zebrafish fin regeneration after cryoinjury-induced tissue damage. *Biology Open*, **5**, 819–828.

Chetty, S.S., Praneetha, S., Govarthanan, K., Verma, R.S. & Murugan, A.V. (2019) Noninvasive tracking and regenerative capabilities of transplanted human umbilical cord-derived mesenchymal stem cells labeled with I-III-IV semiconducting nanocrystals in liver-injured living mice. *ACS Applied Materials & Interfaces*, **11**, 8763–8778.

Cohen, J.E. & MacWilliams, H.K. (1975) The control of foot formation in transplantation experiments with *Hydra viridis*. *Journal of Theoretical Biology*, **50**, 87–105.

Curado, S., Stainier, D.Y.R. & Anderson, R.M. (2008) Nitroreductase-mediated cell/tissue ablation in zebrafish: a spatially and temporally controlled ablation method with applications in developmental and regeneration studies. *Nature protocols*, **3**, 948–954.

Delorme, S.L., Lungu, I.M. & Vickaryous, M.K. (2012) Scar-free wound healing and regeneration following tail loss in the Leopard gecko, *Eublepharis macularius*. *The Anatomical Record*, **295**, 1575–1595.

Dominici, M., Le Blanc, K., Mueller, I., Slaper-Cortenbach, I., Marini, F.C., Krause, D.S., Deans, R.J., Keating, A., Prockop, D.J. & Horwitz, E.M. (2006) Minimal criteria for defining multipotent mesenchymal stromal cells. The International Society for Cellular Therapy position statement. *Cytotherapy*, **8**, 315–317.

Du, Y., Carlson, E.C., Funderburgh, M.L., Birk, D.E., Pearlman, E., Gua, N., Kao, W.W.Y. & Funderburgh, J.L. (2009) Stem cell therapy restores transparency to defective murine corneas. *Stem Cells*, **27**, 1635–1642.

Dufour, J.M., Rajotte, R. V, Korbutt, G.S. & Emerich, D.F. (2003) Harnessing the immunomodulatory properties of Sertoli cells to enable xenotransplantation in type I diabetes. *Immunological Investigations*, **32**, 275–297.

Dym, M. & Fawcett, D.W. (1970) The blood-testis barrier in the rat and the physiological compartmentation of the seminiferous epithelium. *Biology of Reproduction*, **3**, 308–326.

Edwards, J.P., Zhang, X., Frauwirth, K.A. & Mosser, D.M. (2006) Biochemical and functional characterization of three activated macrophage populations. *Journal of Leukocyte Biology*, **80**, 1298–1307.

Engel, F.B., Schebesta, M., Duong, M.T., Lu, G., Ren, S., Madwed, J.B., Jiang, H., Wang, Y. & Keating, M.T. (2005) p38 MAP kinase inhibition enables proliferation of adult mammalian cardiomyocytes. *Genes & Development*, **19**, 1175–1187.

Engel, F.B., Hsieh, P.C.H., Lee, R.T. & Keating, M.T. (2006) FGF1/p38 MAP kinase inhibitor therapy induces cardiomyocyte mitosis, reduces scarring, and rescues function after myocardial infarction. *Proceedings of the National Academy of Sciences of the United States of America*, **103**, 15546–15551.

Fallarino, F., Luca, G., Calvitti, M., Mancuso, F., Nastruzzi, C., Fioretti, M.C., Grohmann, U., Becchetti, E., Burgevin, A., Kratzer, R., Van Endert, P., Boon, L., Puccetti, P. & Calafiore, R. (2009) Therapy of experimental type 1 diabetes by isolated Sertoli cell xenografts alone. *Journal of Experimental Medicine*, **206**, 2511–2526.

Fischer, A.H., Jacobson, K.A., Rose, J. & Zeller, R. (2008) Cryosectioning tissues. *Cold Spring Harbour Laboratory Press*, **3**, https://doi.org/10.1101/pdb.prot4991.

Frangogiannis, N.G., Mendoza, L.H., Lindsey, Merry, L., Ballantyne, C.M., Michael, L.H., Smith, C.W. & Entman, M.L. (2000) IL-10 is induced in the reperfused myocardium and may modulate the reaction to injury. *The Journal of Immunology*, **165**, 2798–2808.

Freyman, T., Polin, G., Osman, H., Crary, J., Lu, M., Cheng, L., Palasis, M. & Wilensky, R.L. (2006) A quantitative, randomized study evaluating three methods of mesenchymal stem cell delivery following myocardial infarction. *European Heart Journal*, **27**, 1114–1122.

Fukazawa, T., Naora, Y., Kunieda, T. & Kubo, T. (2009) Suppression of the immune response potentiates tadpole tail regeneration during the refractory period. *Development*, **136**, 2323–2327.

Gallina, C., Turinetto, V. & Giachino, C. (2015) A new paradigm in cardiac regeneration: the mesenchymal stem cell secretome. *Stem Cells International*, **2015**, http://dx.doi.org/10.1155/2015/765846, (Review).

Garcia-Puig, A., Mosquera, J.L., Jiménez-Delgado, S., García-Pastor, C., Jorba, I., Navajas, D., Canals, F. & Raya, A. (2019) Proteomics analysis of extracellular matrix remodeling during zebrafish heart regeneration. *Molecular & Cellular Proteomics*, **18**, 1745–1755.

Godwin, J.W., Debuque, R., Salimova, E. & Rosenthal, N.A. (2017) Heart regeneration in the salamander relies on macrophage- mediated control of fibroblast activation and the extracellular landscape. *NPJ Regenerative Medicine*, **2**, https://doi.org/10.1038/s41536-017-0027-y.

González-Rosa, J.M., Martín, V., Peralta, M., Torres, M. & Mercader, N. (2011) Extensive scar formation and regression during heart regeneration after cryoinjury in zebrafish. *Development*, **138**, 1663–1674.

Hagège, A.A., Marolleau, J.P., Vilquin, J.T., Alhéritière, A., Peyrard, S., Duboc, D., Abergel, E., Messas, E., Mousseaux, E., Schwartz, K., Desnos, M. & Menasché, P. (2006) Skeletal myoblast transplantation in ischemic heart failure: Long-term follow-up of the first phase I cohort of patients. *Circulation*, **114**, 108–113.

Haubner, B.J., Adamowicz-Brice, M., Khadayate, S., Tiefenthaler, V., Metzler, B., Aitman, T. & Penninger, J.M. (2012) Complete cardiac regeneration in a mouse model of myocardial infarction. *Aging*, **4**, 966–977.

Hay, E.D. & Fischman, D.A. (1961) Origin of the blastema in regenerating limbs of the newt *Triturus viridescens*. *Developmental Biology*, **3**, 26–59.

Head, J.R., Neaves, W.B. & Billingham, R.E. (1983) Immune privilege in the testis. *Transplantation*, **36**, 423–431.

Heallen, T., Zhang, M., Wang, J., Bonilla-Claudio, M., Klysik, E., Johnson, R.L. & Martin, J.F. (2011) Hippo pathway inhibits Wnt signaling to restrain cardiomyocyte proliferation and heart size. *Science*, **332**, 458–461.

Heallen, T., Morikawa, Y., Leach, J., Tao, G., Willerson, J.T., Johnson, R.L. & Martin, J.F. (2013) Hippo signaling impedes adult heart regeneration. *Development*, **140**, 4683–4690.

Herzog, C., Lorenz, A., Gillmann, H.J., Chowdhury, A., Larmann, J., Harendza, T., Echtermeyer, F., Müller, M., Schmitz, M., Stypmann, J., Seidler, D.G., Damm, M., Stehr, S.N., Koch, T., Wollert, K.C., Conway, E.M. & Theilmeier, G. (2014) Thrombomodulin's lectin-like domain reduces myocardial damage by interfering with HMGB1-mediated TLR2 signalling. *Cardiovascular Research*, **101**, 400–410.

Horckmans, M., Ring, L., Duchene, J., Santovito, D., Schloss, M.J., Drechsler, M., Weber, C., Soehnlein, O. & Steffens, S. (2017) Neutrophils orchestrate post-myocardial infarction healing by polarizing macrophages towards a reparative phenotype. *European Heart Journal*, **38**, 187–197.

Hung, S.P., Yang, M.H., Tseng, K.F. & Lee, O.K. (2013) Hypoxia-induced secretion of TGF-beta 1 in mesenchymal stem cell promotes breast cancer cell progression. *Cell Transplantation*, **22**, 1869–1882.

Ieda, M., Tsuchihashi, T., Ivey, K.N., Ross, R.S., Hong, T., Shaw, R.M. & Srivastava, D. (2009) Cardiac fibroblasts regulate myocardial proliferation through beta 1 integrin signaling. *Developmental Cell*, **16**, 233–244.

Ito, K., Morioka, M., Kimura, S., Tasaki, M., Inohaya, K. & Kudo, A. (2014) Differential reparative phenotypes between zebrafish and medaka after cardiac injury. *Developmental Dynamics*, **243**, 1106–1115.

Jaklenec, A., Stamp, A., Deweerd, E., Sherwin, A. & Langer, R. (2012) Progress in the tissue engineering and stem cell industry "are we there yet?" *Tissue Engineering: Part B*, **18**, 155–166.

Jesty, S.A., Steffey, M.A., Lee, F.K., Breitbach, M., Hesse, M., Reining, S., Lee, J.C., Doran, R.M., Nikitin, A.Y., Fleischmann, B.K. & Kotlikoff, M.I. (2012) C-kit + precursors support postinfarction myogenesis in the neonatal, but not adult, heart. *Proceedings of the National Academy of Sciences of the United States of America*, **109**, 13380–13385.

Jopling, C., Sleep, E., Raya, M., Martí, M., Raya, A. & Belmonte, J.C.I. (2010) Zebrafish heart regeneration occurs by cardiomyocyte dedifferentiation and proliferation. *Nature*, **464**, 606–609.

Katsha, A.M., Ohkouchi, S., Xin, H., Kanehira, M., Sun, R., Nukiwa, T. & Saijo, Y. (2011) Paracrine factors of multipotent stromal cells ameliorate lung injury in an elastase-induced emphysema model. *Molecular Therapy*, **19**, 196–203.

Kaur, G., Thompson AL. & Dufour, M. (2014) Sertoli cells- Immunological sentinels of spermatogenesis. *Seminars in Cell and Developmental Biology*, **30**, 36–44, (Review).

Kikuchi, K., Holdway, J.E., Werdich, A.A., Anderson, R.M., Fang, Y., Egnaczyk, G.F., Evans, T., Macrae, C.A., Stainer, D.Y.R. & Poss, K.D. (2010) Primary contribution to zebrafish heart regeneration by gata4+ cardiomyocytes. *Nature*, **464**, 601–605.

King, M.W., Neff, A.W. & Mescher, A.L. (2012) The developing *Xenopus* limb as a model for studies on the balance between inflammation and regeneration. *The Anatomical Record*, **295**, 1552–1561, (Review).

Kjær, I. & Nolting, D. (2009) The human periodontal membrane – focusing on the spatial interrelation between the epithelial layer of Malassez, fibers, and innervation. *Acta Odontologica Scandinavica*, **67**, 134–138.

Kragl, M., Knapp, D., Nacu, E., Khattak, S., Maden, M., Epperlein, H.H. & Tanaka, E.M. (2009) Cells keep a memory of their tissue origin during axolotl limb regeneration. *Nature*, **460**, 60–65.

Kukielka, G.L., Smith, C.W., Manning, A.M., Youker, K.A., Michael, L.H. & Entman, M.L. (1995) Induction of interleukin-6 synthesis in the myocardium. *Circulation*, **92**, 1866–1875.

Lai, S., Marín-Juez, R., Moura, P.L., Kuenne, C., Lai, J.K.H., Tsedeke, A.T., Guenther, S., Looso, M. & Stainer, D.Y. (2017) Reciprocal analyses in zebrafish and medaka reveal that harnessing the immune response promotes cardiac regeneration. *eLife*, **6**, https://doi.org/10.7554/eLife.25605.

Lai, S.L., Marín-Juez, R. & Stainier, D.Y.R. (2019) Immune responses in cardiac repair and regeneration: a comparative point of view. *Cellular and Molecular Life Sciences*, **76**, 1365–1380, (Review).

Landry, Y., Lê, O., Mace, K.A., Restivo, T.E. & Beauséjour, C.M. (2010) Secretion of SDF-1α by bone marrow-derived stromal cells enhances skin wound healing of C57BL/6 mice exposed to ionizing radiation. *Journal of Cellular and Molecular Medicine*, **14**, 1594–1604.

Lee, H.-M., Oh, B.C., Lim, D.-P., Lee, D.-S., Lim, H.-G., Park, S.C. & Lee, J.R. (2008) Mechanism of humoral and cellular immune modulation provided by porcine Sertoli cells. *Journal of Korean Medical Sience*, **23**, 514–520.

Leng, Z., Zhu, R., Hou, W., Feng, Y., Yang, Y., Han, Q., Shan, G., Meng, F., Du, D., Wang, S., Fan, J., Wang, W., Deng, L., Shi, H., Li, H., Hu, Z., Zhang, F., Gao, J., Liu, H., Li, X., Zhao, Y., Yin, K., He, X., Gao, Z., Wang, Y., Yang, B., Jin, R., Stambler, I., Lim, L.W., Su, H., Moskalev, A., Cano, A., Chakrabarti, S., Min, K.-J., Elison-Hughes, G., Caruso, C., Jin, K. & Zhao, R.C. (2020) Transplantation of ACE2 - mesenchymal stem cells improves the outcome of patients with COVID-19 pneumonia. *Aging and Disease*, **11**, 216–228.

Li, Y., He, L., Huang, X., Bhaloo, S.I., Zhao, H., Zhang, S., Pu, W., Tian, X., Li, Y., Liu, Q., Yu, W., Zhang, L., Liu, X., Liu, K., Tang, J., Zhang, H., Cai, D., Ralf, A.H., Xu, Q., Lui, K.O. & Zhou, B. (2018) Genetic lineage tracing of nonmyocyte population by dual recombinases. *Circulation*, **138**, 793–805.

Liao, S., Dong, W., Lv, L., Guo, H., Yang, J., Zhao, H., Huang, R., Yuan, Z., Chen, Y., Feng, S., Zheng, X., Huang, J., Huang, W., Qi, X. & Cai, D. (2017) Heart regeneration in adult *Xenopus tropicalis* after apical resection. *Cell & Bioscience*, **7**, https://doi.org/10.1186/s13578-017-0199-6.

Lim, H.G., Lee, H.M., Oh, B.C. & Lee, J.R. (2009) Cell-mediated immunomodulation of chemokine receptor 7-expressing porcine Sertoli cells in murine heterotopic heart transplantation. *Journal of Heart and Lung Transplantation*, **28**, 72–78.

Lozito, T.P. & Tuan, R.S. (2016) Lizard tail skeletal regeneration combines aspects of fracture healing and blastema-based regeneration. *Development*, **143**, 2946–2957.

Lugrin, J., Parapanov, R., Rignault-Clerc, S., Feihl, F., Waeber, B., Müller, O., Vergely, C., Zeller, M., Tardivel, A., Schneider, P., Liaudet, L., Vergely, C., Zeller, M., Tardivel, A., Schneider, P., Pacher, P. & Liaudet, L. (2015) IL-1 α is a crucial danger signal triggering acute myocardial inflammation during myocardial infarction. *The Journal of Immunology*, **194**, 499–503.

Lv, L., Liao, Z., Luo, J., Chen, H., Guo, H., Yang, J., Huang, R., Pu, Q., Zhao, H., Yuan, Z., Feng, S., Qi, X. & Cai, D. (2020) Cardiac telocytes exist in the adult *Xenopus tropicalis* heart. *Journal of Cellular and Molecular Medicine*, **24**, 2531–2541.

Manabe, I., Shindo, T. & Nagai, R. (2002) Gene expression in fibroblasts and fibrosis involvement in cardiac hypertrophy. *Circulation Research*, **91**, 1103–1113, (Review).

Mao, C. a, Glorioso, J. & Scott, N. (2015) Liver regeneration. *Translational Research*, **163**, 352–362, (Review).

Marshall, L., Vivien, C., Girardot, F., Péricard, L., Demeneix, B.A., Coen, L. & Chai, N. (2017) Persistent fibrosis, hypertrophy and sarcomere disorganisation after endoscopy-guided heart resection in adult *Xenopus*. *PLOS ONE*, **12**, https://doi.org/10.1371/journal.pone.0173418.

Marshall, L.N., Vivien, C.J., Girardot, F., Péricard, L., Scerbo, P., Palmier, K., Demeneix, B.A. & Coen, L. (2019) Stage-dependent cardiac regeneration in *Xenopus* is regulated by thyroid hormone availability. *Proceedings of the National Academy of Sciences of the United States of America.*, **116**, 3614–3623.

Matsui, T., Onouchi, T., Shiogama, K., Mizutani, Y., Inada, K., Yu, F., Hayasaka, D., Morita, K., Ogawa, H., Mahara, F. & Tsutsumi, Y. (2015) Coated glass slides TACAS are applicable to heat-assisted immunostaining and in situ hybridization at the electron microscopy level. *Acta Histochemica et Cytochemica*, **48**, 153–157.

Meisel, R., Zibert, A., Laryea, M., Göbel, U., Däubener, W. & Dilloo, D. (2004) Human bone marrow stromal cells inhibit allogeneic T-cell responses by indoleamine 2,3-dioxygenase-mediated tryptophan degradation. *Blood*, **103**, 4619–4621.

Mohammadi, M.M., Kattih, B., Grund, A., Froese, N., Korf-Klingebiel, M., Gigina, A., Schrameck, U., Rudat, C., Liang, Q., Kispert, A., Wollert, K.C., Bauersachs, J. & Heineke, J. (2017) The transcription factor GATA 4 promotes myocardial regeneration in neonatal mice. *EMBO Molecular Medicine*, **9**, 265–279.

Mosqueira, D., Pagliari, S., Uto, K., Ebara, M., Romanazzo, S., Escobedo-Lucea, C., Nakanishi, J., Taniguchi, A., Franzese, O., Nardo, P. Di, Goumas, M.J., Traversa, E., Pinto-do-Ó, P., Aoyagi, T. & Forte, G. (2014) Hippo pathway effectors control cardiac progenitor cell fate by acting as dynamic sensors of substrate mechanics and nanostructure. *ACS Nano*, **8**, 2033–2047.

Nagahashi, M., Shimada, Y., Ichikawa, H., Nakagawa, S., Sato, N., Kaneko, K., Homma, K., Kawasaki, T., Kodama, K., Lyle, S., Takabe, K. & Wakai, T. (2017) Formalin-fixed paraffin-embedded sample conditions for deep next generation sequencing. *Journal of Surgical Research*, **220**, 125–132.

Németh, K., Leelahavanichkul, A., Yuen, P.S.T., Mayer, B., Parmelee, A., Doi, K., Robey, P.G., Leelahavanichkul, K., Koller, B.H., Brown, J.M., Hu, X., Jelinek, I., Star, R.A. & Mezey, É. (2009) Bone marrow stromal cells attenuate sepsis via prostaglandin E 2-dependent reprogramming of host macrophages to increase their interleukin-10 production. *Nature Medicine*, **15**, 42–49.

Nguyen, T.M.X. (2019) The study of *Xenopus tropicalis* testis-derived stem cells. *Doctoral Dissertation*, Charles University, Czech Republic.

Nguyen, T.M.X., Vegrichtova, M., Tlapakova, T., Krulova, M. & Krylov, V. (2019) Epithelial-mesenchymal transition promotes the differentiation potential of *Xenopus tropicalis* immature Sertoli cells. *Stem Cells International*, **8387478**, https://doi.org/10.1155/2019/8387478.

O'Bryan, M.K., Gerdprasert, O., Nikolic-Paterson, D.J., Meinhardt, A., Muir, J.A., Foulds, L.M., Phillips, D.J., De Kretser, D.M. & Hedger, M.P. (2005) Cytokine profiles in the testes of rats treated with lipopolysaccharide reveal localized suppression of inflammatory responses. *American Journal of Physiology - Regulatory Integrative and Comparative Physiology*, **288**, 1744–1755.

Panahi, S., Karamian, A., Sajadi, E., Aliaghaei, A., Nazarian, H., Abdi, S., Danyali, S., Paktinat, S., Abdollahifar, M.-A. & Farahani, R.M. (2020) Sertoli cell – conditioned medium restores spermatogenesis in azoospermic mouse testis. *Cell and Tissue Research*, **379**, 577–587.

Porrello, E.R. & Olson, E.N. (2014) A neonatal blueprint for cardiac regeneration. *Stem Cell Research*, **13**, 556–570, (Review).

Porrello, E.R., Mahmoud, A.I., Simpson, E., Hill, J.A., Richardson, J.A., Olson, E.N. & Sadek, H.A. (2011) Transient regenerative potential of the neonatal mouse heart. *Science*, **331**, 1078–1080.

Porrello, E.R., Mahmoud, A.I., Simpson, E., Johnson, B.A., Grinsfelder, D. & Canseco, D. (2013) Regulation of neonatal and adult mammalian heart regeneration by the miR-15 family. *Proceedings of the National Academy of Sciences of the United States of America*, **110**, 187–192.

Poss, K.D., Wilson, L.C. & Keating, M.T. (2002) Heart regeneration in zebrafish. *Science*, **298**, 2188–2191.

Rao, J., Yue, S., Fu, Y., Zhu, J., Wang, X., Busuttil, R., Kupiec-Weglinski, J., Lu, L. & Zhai, Y. (2014) Activating transcription factor 6 mediates a pro-inflammatory synergy between ER stress and TLR activation in the pathogenesis of liver ischemia reperfusion injury. *American Journal of Transplantation*, **14**, 1552–1561.

Reimer, M.M., Sorensen, I., Kuscha, V., Frank, R.E., Liu, C., Becker, C.G. & Becker, T. (2008) Motor neuron regeneration in adult zebrafish. *The Journal of Neurosience*, **28**, 8510–8516.

Ren, G., Zhang, L., Zhao, X., Xu, G., Zhang, Y., Roberts, A.I., Zhao, R.C. & Shi, Y. (2008) Mesenchymal stem cell-mediated immunosuppression occurs via concerted action of chemokines and nitric oxide. *Cell Stem Cell*, **2**, 141–150.

Riley, J.K., Takeda, K., Akira, S. & Schreiber, R.D. (1999) Interleukin-10 receptor signaling through the JAK-STAT pathway. *Journal of Biological Chemistry*, **274**, 16513–16521.

Rumyantsev, P.P. (1973) Post-injury DNA synthesis, mitosis and ultrastructural reorganization of adult frog cardiac myocytes. An electron microscopic-autoradiographic study. *Zeitschrift für Zellforschung und Mikroskopische Anatomie*, **139**, 431–450.

Sahraian, M.A., Bonab, M.M., Mohammad, S., Owji, M. & Moghadasi, A.N. (2019) Therapeutic use of intrathecal mesenchymal stem cells in patients with multiple sclerosis : A pilot study with booster injection. *Immunological Investigations*, **48**, 160–168.

Sanberg, P.R., Borlongan, C. V, Saporta, S. & Cameron, D.F. (1996) Testis-derived Sertoli cells survive and provide localized immunoprotection for xenografts in rat brain. *Nature Biotechnology*, **14**, 1692–1695.

Sandoval-Guzmán, T., Wang, H., Khattak, S., Schuez, M., Roensch, K., Nacu, E., Tazaki, A., Joven, A., Tanaka, E.M. & Simon, A. (2014) Fundamental differences in dedifferentiation and stem cell recruitment during skeletal muscle regeneration in two salamander species. *Cell Stem Cell*, **14**, 174–187.

Satoh, A., Suzuki, M., Amano, T., Tamura, K. & Ide, H. (2005) Joint development in *Xenopus laevis* and induction of segmentations in regenerating froglet limb (spike). *Developmental Dynamics*, **233**, 1444–1453.

Senyo, S.E., Steinhauser, M.L., Pizzimenti, C.L., Yang, V.K., Cai, L., Wang, M., Wu, T., Guerquin-Kern, J.L., Lechene, C.P. & Lee, R.T. (2013) Mammalian heart renewal by pre-existing cardiomyocytes. *Nature*, **493**, 433–436.

Shabbir, A., Zisa, D., Suzuki, G. & Lee, T. (2009) Heart failure therapy mediated by the trophic activities of bone marrow mesenchymal stem cells: a noninvasive therapeutic regimen. *American Journal of Physiology-Heart and Circulatory Physiology*, **296**, 1888–1897.

Shi, S., Cote, R.J. & Taylor, C.R. (2001) Antigen retrieval techniques: current perspectives. *The Journal of Histochemistry & Cytochemistry*, **49**, 931–937, (Review).

Shim, K. (2011) Vibratome sectioning for enhanced preservation of the cytoarchitecture of the mammalian organ of corti. *Journal of Visualized Experiments*, **52**, https://doi.org/10.3791/2793.

Sousa, S., Afonso, N., Bensimon-Brito, A., Fonseca, M., Simões, M., Leon, J., Roehl, H., Cancela, M.L. & Jacinto, A. (2011) Differentiated skeletal cells contribute to blastema formation during zebrafish fin regeneration. *Development*, **138**, 3897–3905.

Stawowy, P., Margeta, C., Kallisch, H., Seidah, N.G., Chrétien, M., Fleck, E. & Graf, K. (2004) Regulation of matrix metalloproteinase MT1-MMP/MMP-2 in cardiac fibroblasts by TGF-β1 involves furin-convertase. *Cardiovascular Research*, **63**, 87–97.

Syrjänen, S. & Syrjänen, K. (1986) An improved in situ DNA hybridization protocol for detection of human papillomavirus (HPV) DNA sequences in paraffin-embedded biopsies. *Journal of Virological Methods*, **14**, 293–304.

Taguchi, O., Cunha, R., Lawrence, W.D. & Robboyq, S.J. (1984) Timing and irreversibility of Müllerian duct inhibition in the embryonic reproductive tract of the human male. *Developmental Biology*, **106**, 394–398.

Thornton, C.S. (1960) Influence of an eccentric epidermal cap on limb regeneration in *Amblystoma* larvae. *Developmental Biology*, **2**, 551–569.

Timmers, L., Kiang Lim, S., Hoefer, I.E., Arslan, F., Chai Lai, R., van Oorschot, A.A.M., Goumans, J.M., Strijder, C., Kwan Sze, S., Choo, A., Piek, J.J., Doevendans, P.A., Pasterkamp, G. & de Kleijn, D.P.V. De. (2011) Human mesenchymal stem cell-conditioned medium improves cardiac function following myocardial infarction. *Stem Cell Research*, **6**, 206–214.

Tlapakova, T., Nguyen, T.M.X., Vegrichtova, M., Sidova, M., Strnadova, K., Blahova, M. & Krylov, V. (2016) Identification and characterization of *Xenopus tropicalis* common progenitors of Sertoli and peritubular myoid cell lineages. *Biology Open*, **5**, 1275–1282.

Toma, C., Wagner, W.R., Bowry, S., Schwartz, A. & Villanueva, F. (2009) Fate of culture-expanded mesenchymal stem cells in the microvasculature: *in vivo* observations of cell kinetics. *Circulation Research*, **104**, 398–402.

Uchinaka, A., Kawaguchi, N., Mori, S., Hamada, Y., Miyagawa, S., Saito, A., Sawa, Y. & Matsuura, N. (2014) Tissue inhibitor of metalloproteinase-1 and -3 improves cardiac function in an ischemic cardiomyopathy model rat. *Tissue Engineering: Part A*, **20**, 3073–3084.

Vihtelic, T.S. & Hyde, D.R. (2000) Light-induced rod and cone cell death and regeneration in the adult albino zebrafish (*Danio rerio*) retina. *Journal of Neurobiology*, **44**, 289–307.

Wan, E., Yeap, X.Y., Dehn, S., Terry, R., Novak, M., Zhang, S., Iwata, S., Han, X., Homma, S., Drosatos, K., Lomasney, J., Engman, D.M., Miller, S.D., Vaughan, D.E., Morrow, J.P., Kishore, R. & Thorp, E.B. (2013) Enhanced efferocytosis of apoptotic cardiomyocytes through myeloid-epithelial-reproductive tyrosine kinase links acute inflammation resolution to cardiac repair after infarction. *Circulation Research*, **113**, 1004–1012.

Wang, J., Panáková, D., Kikuchi, K., Holdway, J.E., Gemberling, M., Burris, J.S., Singh, S.P., Dickson, A.L., Lin, Y., Sabeh, M.K., Werdich, A.A., Yelon, D., Macrae, C.A. & Poss, K.D. (2011) The regenerative capacity of zebrafish reverses cardiac failure caused by genetic cardiomyocyte depletion. *Development*, **138**, 3421–3430.

Ward, T.S., Rosen, G.D. & Von Bartheld, C.S. (2008) Optical disector counting in cryosections and vibratome sections underestimates particle numbers: effects of tissue quality. *Microscopy Research and Technique*, **71**, 60–68.

Webster, J.D., Miller, M.A., Dusold, D. & Ramos-Vara, J. (2009) Effects of prolonged formalin fixation on diagnostic immunohistochemistry in domestic animals. *The Journal of Histochemistry & Cytochemistry*, **57**, 753–761.

Wojdasiewicz, P., Poniatowski, Ł.A. & Szukiewicz, D. (2014) The role of inflammatory and anti-inflammatory cytokines in the pathogenesis of osteoarthritis. *Mediators of Inflammation*, **561459**, http://dx.doi.org/10.1155/2014/561459, (Review).

Wollina, U., Schreiber, G., Gornig, M., Feldrappe, S., Burchert, M. & Gabius, H.-J. (1999) Sertoli cell expression of galectin-1 and -3 and accessible binding sites in normal human testis and Sertoli cell only-syndrome. *Histology and Histopathology*, **14**, 779–784.

World Health Organisation. (2018) The top 10 causes of death: Fact sheet, https://www.who.int/news-room/fact-sheets/detail/the-top-10-causes-of-death.

Xin, M., Kim, Y., Sutherland, L.B., Murakami, M., Qi, X., Mcanally, J., Porrello, E.R., Mahmoud, A.I., Tan, W., Shelton, J.M., Richardson, J.A., Sadek, H.A., Bassel-Duby, R. & Olson, E.N. (2013) Hippo pathway effector Yap promotes cardiac regeneration. *Proceedings of the National Academy of Sciences of the United States of America*, **110**, 13839–13844.

Yang, E. V., Gardiner, D.M., Carlson, M.R.J., Nugas, C.A. & Bryant, S. V. (1999) Expression of Mmp-9 and related matrix metalloproteinase genes during axolotl limb regeneration. *Developmental Dynamics*, **216**, 2–9.

Yang, J., Yang, F., Campos, L.S., Mansfield, W., Skelton, H., Hooks, Y. & Liu, P. (2017) Quenching autofluorescence in tissue immunofluorescence. *Wellcome Open Research*, **2**, https://doi.org/10.12688/wellcomeopenres.12251.1.

Ylostalo, J.H., Bartosh, T.J., Coble, K. & Prockop, D.J. (2012) Human mesenchymal stem/stromal cells (hMSCs) cultured as spheroids are self-activated to produce prostaglandin E2 (PGE2) that directs stimulated macrophages into an anti-inflammatory phenotype. *Stem Cells*, **30**, 2283–2296.

Yokonishi, T., Mckey, J., Ide, S. & Capel, B. (2020) Sertoli cell ablation and replacement of the spermatogonial niche in mouse. *Nature Communications*, **11**, https://doi.org/10.1038/s41467-019-13879-8.

Yu, J.K., Sarathchandra, P., Chester, A., Yacoub, M., Brand, T. & Butcher, J.T. (2018) Cardiac regeneration following cryoinjury in the adult zebrafish targets a maturation-specific biomechanical remodeling program. *Scientific Reports*, **8**, https://doi.org/10.1038/s41598-018-33994-8.

Yuan, F., Xiong, G., Cohen, N.A. & Cohen, A.S. (2017) Optimized protocol of methanol treatment for immunofluorescent staining in fixed brain slices. *Applied Immunohistochemistry & Molecular Morphology*, **25**, 221–224.

Zeisberg, E.M., Ma, Q., Juraszek, A.L., Moses, K., Schwartz, R.J., Izumo, S. & Pu, W.T. (2005) Morphogenesis of the right ventricle requires myocardial expression of *Gata4*. *Journal of Clinical Investigation*, **115**, 1522–1531.

Zhang, M., Yang, L., Yuan, F., Chen, Y. & Lin, G. (2018) Dicer inactivation stimulates limb regeneration ability in *Xenopus laevis*. *Wound Repair and Regeneration*, **26**, 46–53.

Zhang, Y., Zhong, J.F., Qiu, H., Maclellan, W.R., Marbán, E. & Wang, C. (2015a) Epigenomic reprogramming of adult cardiomyocyte-derived cardiac progenitor cells. *Scientific Reports*, **5**, https://doi.org/10.1038/srep17686.

Zhang, Y., Liang, X., Liao, S., Wang, W., Wang, J., Li, X., Ding, Y., Liang, Y., Gao, F., Yang, M., Fu, Q., Xu, A., Chai, Y.-H., He, J., Tse, H.-F. & Lian, Q. (2015b) Potent paracrine effects of human induced pluripotent stem cell- derived mesenchymal stem cells attenuate doxorubicin-induced cardiomyopathy. *Scientific Reports*, **5**, https://doi.org/10.1038/srep11235.

Zhao, L., Liu, X., Zhang, Y., Liang, X., Ding, Y., Xu, Y., Fang, Z. & Zhang, F. (2016) Enhanced cell survival and paracrine effects of mesenchymal stem cells overexpressing hepatocyte growth factor promote cardioprotection in myocardial infarction. *Experimental Cell Research*, **344**, 30–39.